Università degli Studi di Palermo

AREA RICERCA E TRASFERIMENTO TECNOLOGICO
SETTORE DOTTORATI E CONTRATTI PER LA RICERCA
U. O. DOTTORATI DI RICERCA

PhD in Biomedicine, Neurosciences and Advanced Diagnostics.
Department of Biomedicine, Neurosciences and Advanced Diagnostics (BiND)
SSD: MED/27

ADVANCED MOLECULAR DIAGNOSTICS AND COMPUTATIONAL TECHNOLOGY FOR MOVEMENT DISORDERS SURGERY

IL DOTTORE
Dott. GIUSEPPE ROBERTO GIAMMALVA

IL COORDINATORE
Ch.mo Prof. FABIO BUCCHIERI

IL TUTOR
Ch.mo Prof. DOMENICO GERARDO IACOPINO

CICLO XXXVII
ANNO CONSEGUIMENTO TITOLO 2025

To Marta, my comforting morning star in these long, lonely nights, a harbinger of brighter dawns and new breaths of life.

And to Gioele, little dream-chaser, who captured my heart by waving tenderly at the moon.

Acknowledgement

I think the acknowledgements deserve to be placed at the beginning rather than at the end. Thus, I would like to express my deepest gratitude to *Prof. Celeste Caruso Bavisotto* and *Dr. Giovanni Tringali* for their invaluable, rigorous, and continuous support throughout the different phases of this study. I am profoundly grateful to them, as well as to all my past and present colleagues who have supported me in various ways over the years of this work.

1 Introduction

1.1 Common movement disorders: Essential tremor and Parkinson's disease

Among the wide spectrum of movement disorders, tremor is the most common one and it can deeply affect patient's quality of life since it can interfere with work, social life and basic daily activities [1]. By definition, tremor is ad involuntary, rhythmic and oscillatory movement which can represent a feature of different pathologies and movement disorders, such as Essential Tremor (ET) and Parkinson's Disease (PD), which are the two most prevalent ones.

1.1.1 Essential Tremor (ET)

ET is a progressive movement disorder characterized by action tremor affecting upper limbs, which may occasionally involve lower limbs, head and voice. In case of additional neurological symptoms (e.g. dystonia, cognitive impairment, psychiatric disorders, olfactory changes, oculomotor involvement) ET is categorized as "Essential Tremor plus" It may affect both adult and children in familiar presentation and presents the highest incidence within the elderly population [2]. ET prevalence is rated in 0,4 – 3.9% in general population and up to 8% in over-65 years old population without any sexual difference. [3,4]

Since the action tremor with often severe amplitude and the concurrence of other additional neurological symptoms, ET can cause significant disability. In particular, tremor often limits daily activities such as writing and feeding, causing feeling of shame and leading to social exclusion, job change or early retirement in up to 25% of ET patients because of tremor-induced disability [5–8].

Age of onset presents a bimodal distribution; thus, ET can be classified in young onset and old onset; moreover, ET may be further classified into sporadic and familiar forms. Young onset ET frequently presents familiar history of tremor and may be more likely linked to genetic inheritance, although characteristic pathological features of ET seem to be the same of sporadic or old onset forms [9–11].

ET pathophysiology

ET pathophysiology is heterogeneous and not yet well-known. Among the most credited hypotheses, it has been postulated that ET may be the result of a disruption of neuronal central oscillator involving the inferior olivary nucleus and the olivary-cerebellar pathway [12], or a neurodegenerative condition affecting cerebellar cortex with expansion of GluRδ2-dependant cerebellar climbing fibers and disruption in cerebellar oscillatory activity, or depauperation of Purkinje's cells with accumulation of neurofilament, cells swelling with higher number of torpedoes and dendritic reorganization resulting in GABA deficiency, lower inhibition of dentate nucleus and a disruption of dentato-rubro-thalamic pathway (cerebellar variant of ET), or a neurodegenerative condition affecting locus

coeruleus by accumulation of Lewy's bodies (Lewy body variant of ET – LBVET), or the involvement of β-carboline alkaloids exposure and harmane and harmaline metabolism which may alter cerebellar metabolism affecting olivary-cerebellar tracts [10,12–18]

Despite sporadic forms of ET which present as idiopathic condition, in up to 50-70% of cases ET presents as familiar form with an autosomal dominant transmission and incomplete penetrance, influenced by both genetic and environmental factors[19]. As regards genetic influences, three susceptibility loci have been found until now: 3q13 (EMT1), 2p25-22 (EMT2) and 6p23. [20–22]. Moreover, correlations to be confirmed were found with HS-BP3 gene polymorphism, LINGO 1, FUS and TENM4 genes variants. [23–26]

Treatment

Nowadays several medical and surgical treatment have been proposed for ET. In particular, medical treatment relies mostly on primidone and propranolol, which represent the most effective medication capable of reducing tremor amplitude of a certain degree in up to 70% of patients [27–29]. However, despite initial response, some patients require frequent adjustments of medication until become refractory to medical therapy.

In case of severe disabling and medical refractory ET, different neurosurgical procedures have been proposed. In particular, ventralis intermedius (VIM) thalamotomy and VIM thalamic deep brain stimulation (DBS).

VIM thalamic DBS is a surgical procedure consisting in high-frequency electrical stimulation of VIM nucleus through microelectrodes and implanted pulse generator. This technique was firstly adopted for the treatment of Parkinson's disease and then proposed for the treatment of medical refractory ET. It can be safely performed bilaterally with satisfactory effectiveness, with up to 83% reduction rate of tremor [30]. Standard target of thalamic DBS for ET is the VIM nucleus; however different targets have been proposed with comparable results [31].

DBS is generally considered a safe and effective procedure for the treatment of ET, as the stimulation is adjustable upon patient's response; however it represents a major and long surgical procedure, it is a prosthetic surgery requiring implantation of brain microelectrodes and pulse generator which are prone to long-term malfunctions and infections and it expose patients to risk of neurosurgical complications including bleeding, brain hemorrhage and post-surgical seizures [32,33].

Moreover, despite the initial efficacy of VIM stimulation, a progressive *tremor relapse* may show in up to 70% of ET patients. This phenomenon, described as *tolerance* or *habituation*, can occur already in the first weeks after the optimization of electrical stimulation.[34] : The underlying mechanism of habituation has not been yet completely understood: among the most credited hypotheses are brain adaptation to chronic electrical stimulation, adaptation of thalamo-cerebellar pathway and loss of the initial micro-lesional effect secondary to the placement of microelectrodes. [35,36]. Unfortunately, despite proposed strategies to prevent habituation, such as implantation of different devices,

alternation of stimulation parameters and optimization of concomitant medical therapy, in some patients decrease efficacy of DBS may persists and there is still no effective strategy to prevent or reverse habituation in ET patients undergone DBS. [34–36]

On the other hand, **VIM radiofrequency thalamotomy** is a well-established surgical option for the treatment of ET. It consists in a thermal lesion of the VIM nucleus through the temporary insertion of RF stereotactic electrodes and subsequent thalamic ablation, with immediate effects on tremor [37].

RF VIM thalamotomy was presented as and effective surgical treatment for medical refractory ET even before the introduction of DBS. In facts it shows a long-term effectiveness in up to 70% of patients with significant reduction of tremor rate. Better results on long term outcome and tremor control have been achieved with the aid of advanced neuroimaging techniques such as thalamic segmentation and diffusion tensor tractography; however, tremor can relapse in 15 – 33% of patients within first six months after the treatment despite an initial good post-operative response [38–41]. Despite, RF thalamotomy is less expensive than DBS and require no permanent hardware, it presents potential operative and post-operative neurological complications such as brain hemorrhage, sensory disturbances, hemiparesis, dysarthria, ataxia, gait disturbances, confusion, cognitive decline, some of which present a higher odd in case of bilateral thalamic lesion thus preventing concomitant bilateral RF thalamotomy. [42]

Along with RF thalamotomy, **Gamma Knife (GK) radiosurgery** has been described as alternative and effective technique of VIM thalamotomy for the treatment of ET with comparable result and outcomes, but different post-operative risks such as radiation exposure and delayed onset of clinical effects on tremor which prevents surgeon to properly adapt thalamic lesioning upon patient intraoperative neurological response [43]

Regardless of the treatment, several studies documented reduction in the clinical benefit and *tremor recurrence over time*, even in the case of a good initial response, mostly because of habituation and disease progression tremor recurrence. In case of VIM DBS for the treatment of ET, in as been reported a waning benefit with tremor recurrence in a variable percentage of 36%-73% of ET patients over long term follow up despite the best device set-up [44–50]. In case of tremor recurrence after thalamotomy, reoperation may be an effective choice in case of early recurrences likely due to small lesions, however patients may always present late recurrences due to disease progression [51].

1.1.2 Parkinson’s disease (PD)

Parkinson's disease (PD) is a progressive neurodegenerative disorder which has a large social impact because of its prevalence and clinical implications. It is a slow progressing condition which is clinically characterized by motor symptoms such as bradykinesia, rigidity, and resting tremor. PD is caused by a selective degeneration of dopaminergic neurons in the substantia nigra pars compacta, resulting in dopamine depletion in the striatum, and involving both dopaminergic and non-

dopaminergic circuits. The involvement of non-dopaminergic circuits is related to PD non-motor symptoms such as decreased facial expression, sleep disturbances, decreased sense of smell, psychiatric disorders such as depression and anhedonia, rapid eye movement behavior disorder (RBD) and dysautonomia.[52–54]

Clinical presentation of PD may vary among patients as well as its progression during time. This clinical variability, the degenerative behavior and the disease duration which may span decades, account for PD social, working and familiar burden. [53]

As regards pathology, PD is sustained by accumulation of α-synuclein in Lewy bodies. Typical cytological characteristics, such as vesicular structures, dysmorphic organelles and mitochondria, high lipid content may be found also in other organs, as PD represents not only a neurodegenerative disease but also a multisystem disease. [55,56]

PD affects approximately 1-2% of general population over 65 years and its incidence usually increases with age, typically with a higher prevalence in the late adulthood without any remarkable epidemiological differences worldwide. Its incidence is estimated in up to 21 cases per 100.000 per year with a mean prevalence of 120 cases per 100.000 inhabitant.[57]

However, age at onset may be younger than 65 years old in up to 25% of patients. [57] PD affects both sexes, although women present a higher age at onset and higher risk of psychiatric disorders, dyskinesias and motor and non-motor fluctuations during medical therapy,. [58–61]

PD Pathophysiology

Several etiologies have been linked to PD, in particular genetics, environment and interactions thereof. As regards genetics, despite monogenic forms represent a minority of all PD cases, several genes have been linked to PD: in particular several mutations of SNCA, LRRK2, PRKN, PINK1, and GBA genes. These genetic forms of PD present younger age at onset and familiar aggregation, faster progression and prominent motor and non-motor signs.[62–65] As regards environment, exposure to neurotoxin MPTP was historically linked to PD, but also exposure to pesticides and recently COVID-19 have been suspected to be positively linked to PD. Instead, smoking, coffee consumption, NSAID use, high urate levels and physical activity seems to have a protective role against PD development. [66–70]

The pathophysiology of Parkinson's disease results from the accelerated death of dopaminergic neurons, because of the complex interaction among aberrant α-synuclein aggregation, mitochondrial dysfunction, dysfunctional lysosomes, vesicle and synaptic transport and neuroinflammation.[71]

Depletion of nigrostriatal dopaminergic neurons causes a striatal dopamine depletion, thus producing an imbalance between direct and indirect pathways of the basal ganglia, causing ad increasing inhibitory output from the globus pallidus (GPi) and substantia nigra pars reticulata (SNr) resulting in bradykinesia, rigidity and resting tremor.

Tremor is the most common and one of the primary motor symptoms in PD; it shows in up to 75% of patients since disease onset. [53,72] Tremor is a heterogeneous and disabling feature in PD: it is often a rest tremor affecting mostly upper limbs, but it can be also postural or kinetic, stress-sensitive and may affect also lower limb or head and face. [73,74] Tremor may present as the most prominent symptom in the so-called tremor-dominant PD, which show a less aggressive course than hypokinetic PD [75]. Tremor in PD is only partially caused by striatal dopaminergic depletion, in particular by the reduced dopaminergic effect on VIM nucleus which is part of cerebellar-thalamic pathway, and response to dopaminergic agonists is unpredictable[76–79]. Moreover, it has been shows that VIM nucleus presents neuronal groups with oscillatory activity, thus playing the role of intrinsic thalamic pacemaker, along with other oscillatory group of neurons located in internal globus pallidus (GPi) and subthalamic nucleus (STN); which may be stimulated by afferent proprioceptive input from spino-cerebellar-thalamo-cortical loops. [80–85] Basing on these evidences and according to the "*dimmer-switch model*" tremor in PD originates in the basal ganglia within basal ganglia-cortical loop and it is modulated by cerebello-thalamo-cortical circuits. [86]

Treatment

Historically, pharmacological treatment of PD relies on L-DOPA, combined with dopa-decaboxylase inhibitor in order to prevent dopamine peripheral metabolism. Although L-DOPA represents the most effective medication capable of reducing rigidity, bradykinesia and tremor, it is prone to several direct and indirect side effects, such as late dyskinesias and motor fluctuations mostly in younger patients; slow-releasing formulation of dopamine agonists have been also producer in order to reduce motor fluctuation. The association with catechol-o-methyltransferase (COMT) inhibitor has been proposed as an effective adjunct in order to reduce the "off" periods such as the association with adenosine A2 receptor antagonists, whereas the association with monoamine oxidase-B (MAO-B) inhibitors have been propose as an adjunct for reducing motor fluctuations and amantadine has been largely adopted for the treatment of late dyskinesias despite its risk of hallucinations and corneal edema [87,88].

Along with L-DOPA, dopamine agonists have been proposed as effective adjunct therapy in the early stage of PD; however, their side effects are more common than L-DOPA and include hallucinations, orthostatic hypotension, excessive sleepiness and impulse control disorders; moreover, patients may experience a dopamine agonist withdrawal syndrome because of dopamine agonists reduction, which is characterized by severe psychiatric features such as anxiety, panic, dysphoria and suicidal ideation [87].

Anticholinergic drugs have also been adopted for the treatment of tremor, but their side effects such as confusion, hallucinations, constipation and urinary retention and the increased risk of dementia relegate anticholinergic as second choice medications [87]

Unfortunately, tremor may persist despite multiple medications, along with several side effects from medications and late-onset of dyskinesias during the treatment with L-DOPA. In these cases, surgery is needed in order to reduce medications and to ameliorate patient's symptoms and quality of life.

Surgical treatment of PD is based on ablative techniques such as RF thalamotomy and DBS. **DBS** technique for PD is the same as for ET, however target may differ depending on PD clinical presentation and most prominent symptoms. Primary indications to DBS for PD are uncontrolled motor fluctuations, dyskinesias and tremor, moreover it has been reported that DBS effectiveness on motor-symptoms is persistent for years [87,89,90]. STN and GPi are the most common DBS target for the treatment of PD, the former mostly chosen for the treatment of motor-symptoms and the latter for the treatment of L-DOPA-induced dyskinesias. VIM is a less common target for DBS since its effectiveness is only limited to tremor, thus it is the preferable choice only in case of tremor-dominant PD or as salvage treatment after unsuccessful monolateral thalamotomy or in case of bilateral treatment [87,91–94].

However, DBS present some contraindication for the treatment of PD such as dementia, L-DOPA unresponsive symptoms and unstable psychiatric disorder. Moreover, DBS is prone to complications and side effects: among surgical complications it has been reported an infection rate up to 3%, an intracranial hemorrhage rate of 2% and lead malfunction of 2%; as regard stimulation-related side effects, sensitive symptoms, visual impairment, dysarthria, gait disturbance and cognitive and psychiatric disorders have been reported [95,96].

Along with DBS, in recent years **tcMRgFUS thalamotomy** has emerged as safe and effective technique for the treatment of tremor-dominant PD [97].

1.1.3 Tremor-related disability and quality of life

Both ET and PD are associated with severe disability and a significant reduction in patient's quality of life. In particular, tremor may interfere with basic daily activities such as writing, drinking, dressing or self-caring, resulting in impaired self-sufficiency and increasing dependance. [98,99] Moreover, tremor burden reflects also in professional activities, social and relational life, causing stigmatization, physical discomfort, social embarrassment and isolation: up to 20% of ET and PD patients develop anxiety and depression, psychological distress and decreased sense of security; these effects are inevitably related to patient's subjective perception of tremor severity and self-reported quality of life. [98,100,101]

According to these evidences, in case of medical refractory tremor surgical interventions is deemed mandatory and often required by patients themselves in order to reduce tremor rate, thus determining a substantial improvement in autonomy, reduction in social isolation and embarrassment and improvement of overall quality of life, although no surgical intervention and techniques has been demonstrated free from the possibility of tremor recurrence. [102]

1.1.4 tcMRgFUS VIM thalamotomy for medical refractory tremor

In recent years, **transcranial Magnetic Resonance-guided Focused Ultrasound (tcMRgFUS)** has been being increasingly adopted as lesioning technique along with RF thalamotomy and GK thalamotomy for the treatment of movement disorders, including ET and tremor-dominant PD [43,97,103,104] . TcMRgFUS is a novel, non-invasive technique which adopts high energy focused ultrasound (HI-FU) to produce a sharp and localized lesion onto a certain target volume through the intact skin and skull by direct heating, cavitation and shear stress, using MRI for anatomical imaging and real-time thermal mapping[105–108]. In literature, VIM is the target of choice for tcMRgFUS thalamotomy both for et and tremor-dominant PD and clinical outcomes of tcMRgFUS VIM thalamotomy are comparable to RF thalatomomy and DBS. [109,110]. However, tcMRgFUS is only still approved by FDA for unilateral VIM thalamotomy, which is the target of choice for ET but a favorable target only for tremor in case of PD [87,111]. Nowadays, tcMRgFUS VIM thalamotomy is considered as an effective technique for the treatment of ET and tremor-dominant PD with a significative post-operative improvement on tremor both in ET and in PD series [97,112,113].

Although the profile of adverse events of tcMRgFUS is similar to RF thalamotomy with up to 4% rate of severe adverse events, it is less invasive since it avoids radiation exposure, prevents risk of infection, reduces the risk of bleeding and uncontrolled heating damage to surrounding tissue.[114,115]

Despite the initial effectiveness in tremor rate, tremor may frequently recur after a successful tcMRgFUS thalamotomy both in ET and PD patients: as previously stated for other surgical techniques, the pathophysiological mechanism underlying tremor recurrence is still unknown. [115–117]. In particular, it has been recently demonstrated in a comprehensive meta-analysis that greatest reduction in tremor is achieved within 1 month after tcMRgFUS thalamotomy, but a statistically significant decrease of tcMRgFUS effect is generally seen between 3 and 6 months in over 20% of patients, often equaling and seldomly exceeding pre-operative tremor rate [118–120]. Three hypotheses emerge among the postulated ones: an efficient healing or remyelination of the targeted neural circuit, small lesion for a given target or inappropriate targeting for a given movement disorder. Beyond these hypotheses, movement disorder may progress after tcMRgFUS as neurodegenerative disease, thus inducing the activation of others functional circuit which nullify the previous target lesion [121]. It has been shown that among all patients undergone tcMRgFUS thalamotomy for movement disorder, tremor recurrence is more frequent in case of PD or long-standing ET [117,120,122–124]. Moreover, lesion size, shape and location have been investigated as early radiological predictor of tremor outcome along with post-operative DWI changes and DTI metrics of dentato-rubro-thalamic tract [125–128]. Unfortunately, nowadays reliable clinical or radiological predictors of outcome and tremor recurrence after tcMRgFUS as movement disorder surgery still lack.

1.2 ET and PD molecular pathology: role of Heat Shock Proteins (HSPs) in neurodegeneration

Parkinson's disease represents a neurodegenerative disorder characterized by progressive dopamine depletion. The main molecular pathogenic mechanism is the intracellular accumulation of misfolded alpha-synuclein, which can act in a prion-like manner forming the so-called Lewy bodies. [129,130] Impaired ubiquitine-proteasome system reduces the clearance of misfolded proteins thus promoting the accumulation of alpha-synuclein. [131]

Since the fundamental pathogenic mechanism in PD is an impaired intracellular proteostasis, the involvement of Heat Shock Proteins (HSPs) has been largely investigated during the last years both as pathogenic factors and potential therapeutic targets [132]. HSPs are a heterogeneous family of highly conserved molecular chaperones, which facilitate the correct folding of proteins, prevent their aggregation and promote the degradation of damaged or misfolded ones [131]. Recent studies have enlightened that several HSPs are negatively regulated or under-expressed in brain of PD patients. Among these, HSP27, HSP40, HSP60, HSP70, HSP90, and HSP110 have been particularly investigated since their link with the modulation of alpha-synuclein and neuronal survival. [129,133] In particular, it has been shown that these HSPs are capable of binding to alpha-synuclein and inhibit the formation of Lewy bodies, enhancing the degradation of misfolded proteins through proteasome pathway and autophagy thus reducing alpha-synuclein toxicity, protecting mitochondrial metabolism thus reducing neuronal oxidative stress and generally maintaining neuronal proteostasis [131,134–136].

Within this family of chaperons, some HSPs have gained particular attention in molecular pathology of PD. In particular, it has been demonstrated that **HSP27** plays a neuroprotective role in several neurodegenerative diseases, including PD, due to its ability to inhibit alpha-synuclein aggregation, to promote its degradation and to enhance cell survival through reducing apoptosis by preventing caspase activation. [137–140]

HSP40 is a member of DnaJ proten family; it acts as HSP70 co-chaperone, facilitating proper protein folding, promoting the ATPase activity of HSP70, facilitating the refolding or degradation of misfolded proteins and preventing the aggregation of alpha-synuclein. Functional disruption of HSP40 members such as DNAJA2 and DNAJB1 has been shown to impair proteostasis and contribute to neurodegeneration; moreover, mutations in DnaJ family genes have been directly associated with inherited forms of PD, implicating HSP40 in primary pathogenetic mechanisms. [129,132]

Finally, **HSP90** is involved in the regulation of cell survival and protein aggregation. It has been demonstrated that HSP90 contributes to stabilize alpha-synuclein and to regulate signaling pathway related to stress response and cellular survival in PD; in particular, several studies demonstrated a

co-localization of HSP90 with alpha-synuclein; moreover, elevated HSP90 levels in brain of PD patients correlate with high level of alpha-synuclein. [134] Accordingly, selective inhibition of HSP90 seems to reduce protein aggregation and to promote alpha-synuclein degradation in experimental model of PD, suggesting also a potential therapeutic target for PD. [141–145]

Heat Shock Proteins (HSPs) are also involved in the pathophysiology of essential tremor (ET). Recent studies about gene expression in cerebellar tissues of ET patients have highlighted an aberrant regulation HSP40 with mutation of DNAJC13 gene, suggesting a direct involvement in the pathophysiology of ET (He & Wang, 2022) . However, despite these limited evidences and contrarily to PD, literature about molecular pathology of ET is still poor.

1.3 Big data and Artificial Intelligence (AI): toward bioinformatic models for early prediction of patient's outcome

Nowadays, computer sciences are rapidly growing along with artificial intelligence (AI) in support of neurosciences toward a personalized medicine. In particular, among several computational applications, **radiomics** (e.g. mathematical analysis of radiological images by extrapolation of quantitative data) is changing the way neuroimaging is approached, by unveiling plenty of numerical information from medical images beyond what is visible to the naked eye. [148]

Radiomic features (e.g. shape, intensity, texture and geometry) represent a hyper-dimensional space: the use artificial intelligence (AI) such as **machine learning (ML)** algorithms and neural networks allows to exploit this information to refine complex diagnoses, classify pathologies according to their clinical and pathological findings and even predict patient's clinical course.[148,149]

AI algorithm applied to radiomic analysis have already produced promising result in neuro-oncology, both for diagnostic refinement and for prognostic prediction, thanks to the integration of large amount of clinical and numerical data. In particular, AI through machine learning models has been already used for the prediction of overall survival and progression-free survival of patient affected by glioblastoma from radiomic analysis of pre-operative brain MRI, for the prediction of genetic mutations, tumoral grading and response to medical therapy, thus promoting a prompt tailored treatment. [149–151]

AI have been promisingly adopted through ML algorithms also in several other fields of neurosurgery, such as traumatic brain injury (TBI) for the diagnostic prediction of intracranial hypertension and prognostic prediction of patient's outcome, by the integration of radiomic data, clinical data and physiological parameters [152,153]

As regards movement disorders, AI models have been adopted for the diagnosis of PD, with a great accuracy in distinguishing PD patient from healthy controls basing on data from brain fMRI, and for the prognosis of PD by recognizing in advance early sign of cognitive decline.[154,155] Moreover, in the scenario of the movement disorder surgery, radiomic analysis was successfully adopted for the

prediction of motor outcome after STN- DBS for PD with an accuracy up to 82% [156]. As regards essential tremor, ML algorithm was used for predicting tremor improvement after tcMRgFUS thalamotomy basing on post-operative brain fMRI. [157]

These promising results suggest that AI algorithms applied to neuroimaging, clinical data and radiomic analysis may refine diagnosis, improve patient's selection for surgery, provide a multimodal prognostic tool and promote tailored therapies. Unfortunately, many of these algorithms are still experimental since the wide amount of data needed for the training of AI models; thus, generalization is limited by small cohorts and larger multicenter datasets are needed for external validation. However, according to recent literature, a properly modelled and supervised ML algorithm which analyzes radiomics along with different clinical and molecular features may unveil plenty of possibilities in prognosticating patient's outcome in several clinical scenarios in a reproducible way.

2 Objectives

The aim of this research is to assess the applicability of advanced molecular diagnostics and the reliability of computational technology in the evaluation of patient's outcome after movement disorder surgery. This aim will be pursued by evaluating the expression of specific HSPs from peripheral blood and by developing a reproducible artificial intelligence algorithm based on Machine Learning (ML) using radiomics and clinical data of ET and PD patients undergone tcMRgFUS thalamotomy. The purposes of this study are to investigate the involvement of HSPs into the pathophysiology of ET and PD and to identify useful biomarkers and radiological features in the diagnostic setting, for the evaluation of early recurrence and for the prognostication of patient's outcome after movement disorder surgery.

3 Materials and methods

3.1 Study design

This study consists of two different branches. The first branch is a prospective cohort study aimed to **evaluate HSPs expression** in peripheral blood of ET and PD patients undergone tcMRgFUS thalamotomy. The second branch is a retrospective cohort study aimed to **develop and validate a ML algorithm** for the prognostication of patient's outcome from clinical and radiomic data.

3.2 HSPs expression in tcMRgFUS thalamotomy for tremor

3.2.1 Population

Between 2022 and 2023 a group of 27 ET and PD patients admitted to the Unit of Neurosurgery – A.O.U.P. "P. Giaccone" – Department of Biomedicine, Neurosciences and Advanced Diagnostics of the University of Palermo (Italy) underwent tcMRgFUS unilateral thalamotomy for the treatment of medical refractory tremor.

Among this population, for the purpose of this branch of the study, *inclusion criteria* were: completion of tcMRgFUS VIM thalamotomy, complete clinical and neurological follow up and completion of peripheral blood collection at scheduled time as further described. *Exclusion criteria* were incomplete follow up or incomplete blood sampling,

All enrolled patients underwent peripheral blood collection, radiological and clinical/neurological evaluation at scheduled times. In particular, peripheral blood samples was collected at *T0* (the same day of the tcMRgFUS thalamotomy, before the surgical procedure), *T1* (48h post-op), *T2* (1-month post-op).

For each enrolled patient, radiological evaluation was performed through thin-slice gadolinium-contrast brain MRI in order to evaluate the evolution of thalamic lesion, perilesional oedema and lesion healing at T0 (baseline, before the surgical procedure), T1 (48h post-op) and T2 (1-month post-op).

Clinical and neurological evaluations were performed through the administration of the third section *of Unified Parkinson's Disease Rating Scale (UPDRS-III)* in PD patients and *CRST* scales with global score (*CRST*, 0-144) and contralateral-hand score (*Hand*, 0-16) in ET patients at T0 (baseline, before the surgical procedure), T1 (48h post-op) and T2 (1-month post-op).

All patient gave informed consent and this study obtained approval of local Ethical Committee.

3.2.2 tcMRgFUS VIM thalamotomy

All enrolled patient underwent tcMRgFUS unilateral thalamotomy for the treatment of medical refractory tremor. Left VIM thalamic nucleus was the target of choice both for ET and PD patients, since right arm resulted the most affected and disabling side for all the enrolled patients.

During pre-operative course, each patient underwent brain CT scan and MRI, which were co-registered and used for the proper planning of the procedure in order to mark no-pass regions, to calculate the available head surface, the number of transducers to be employed and the required energy to be delivered during the procedure.

VIM position was calculated on pre-operative brain MRI images by canonical stereotaxic coordinates: anterior to the posterior commissure (PC) by 1/3 of Anterior Commissure – Posterior Commissure (AP-PC) line, 12-14mm laterally from the median plane and 0-2 mm cranially from the intercommisural plane. Targeting was further refined for each patient during mock sonication according to patient's clinical response.

tcMRgFUS thalamotomy was performed at University of Palermo by the use of ExAblate 4000 (InSightec lts – Haifa, Israel) which is made of a hemispheric helmet with 1024-element phased array transducers operating at 650kHz. Patient scalp was shaved prior to procedure, fixed in a stereotactic frame and sealed by silicon membrane with embedded dedicated coils. The helmet was fixed to the stereotactic frame and filled with degassed circulating chill water ensuring an optimal acoustic coupling between transducers and patient scalp. During the procedure patient's vital signs were constantly monitored and patients and both monitoring and operating physicians could immediately stop the sonication by pressing an emergency button.

Sequential intraoperative brain MRI were performed before the procedure, during sonications and at the end of the procedure and were co-registered with the pre-operative brain MRI and CT scan in order to align target coordinates to the actual patient's coordinates. Fiducial markers were placed on live MRI in order to ensure automatic patient's movement detection. Before starting the procedure, a tracking scan was run to verify and register the transducer home position, and the central MRI frequency was verified. Transducers focal point, MRI system alignment and proper targeting were tested by short low-energy sonications (<250W). Once the targeting was confirmed, energy of focused ultrasound beam was gradually increased in order to achieve a temperature between 50°-54°C which produces a transient clinical effect. During this phase, stereotactic coordinates could be modified in order to achieve the best clinical effect on tremor without any side effect. Once the optimal target was confirmed, energy was again increased to achieve focal temperature higher than 55°C in order to obtain a permanent lesion. A final brain MRI was performed for each patient in order to visualize the resulting thalamic lesion.

After the procedure, each patient undergone neurological examination and clinical observation for any delayed post-operative side effect, 48h post-operative brain MRI and then discharged. Neither steroid nor osmotic treatment were administered after the treatment and hospital discharge.

3.2.3 Peripheral blood sampling and processing

To assess the plasma levels of HSP27, HSP40, and HSP90, peripheral blood samples from enrolled ET and PD patients were collected at T0 (the same day as the tcMRgFUS thalamotomy, before the surgical procedure), T1 (48 hours post-op), and T2 (1-month post-op). ELISA immunoassay was performed according to the manufacturer's instructions (Human HSP27 ELISA Kit, Catalog Number: orb561761; Human Heat Shock Protein 40 ELISA Kit, Catalog Number: orb775355; Human HSP90 ELISA Kit, Catalog Number: orb779144. Biorbyt – Cambridge, UK). HSPs plasmatic levels were tested in order to assess a potential variability during follow up after tcMRgFUS thalamotomy and then statistically compared with the results of clinical/neurological evaluations in order to assess a potential correlation between HSPs expression clinical outcome of ET and PD patients.

Briefly, the plasma samples were centrifuged for 15 minutes at 1000×g at 2-8°C. 100 µl of each standard dilutions, prepared according to the instructions, and 100 µl of each sample were added to the 96-well plate precoated with the anti-HSP27/HSP40/HSP90 antibody and incubated for 80' at 37°C. Each standard and each sample were added twice. After two washes, 100 µl of the biotin-labeled antibody working solution was added into each well and incubated for 50' at 37 °C. Subsequently, after three washes, 100 µl of the HRP-Streptavidin Conjugate working solution was added to each well and incubated for 50' at 37°C. At the end, after five washes, 90 µl of the 3,3′, 5,5′-tetramethylbenzidine (TMB) substrate solution was added to each well and incubated for 20 minutes at 37 °C in the dark before stopping the reaction and reading the O.D. absorbance at 450 nm with an appropriate microplate reader.

3.2.4 Statistical analysis

Statistical analysis was performed using R and its graphical interface Jamovi (v 2.6.44.0). Numerical data (HSP27, HSP40, HSP90, global CRTS, hand sub-score of CRST, UPDRS) was tested for normality distribution by Shapiro-Wilk test. Since several variables showed a non-normal distribution ($p<0.05$), non-parametric tests were used for further statistical analysis.

Variation of HSPs serum level and clinical score over time was testes by the Friedman test for repeated measures and paired samples. In case of significative results ($p<0.05$), HSPs levels were compared in pair over time (T0 vs T1, T0 vs T2, T1 vs T2) by Durbin-Conover post-hoc tests. Association between variation of each HSP serum level (ΔHSP) and clinical score (ΔCRST, ΔHand, ΔUPDRS) over time was tested by Spearman correlation considering variation at 48 hours (ΔT1-T0), at one month after the procedure from baseline (ΔT2-T0) and from early post-operative period (ΔT2-T1).

Predictive value of HSPs variation on clinical outcome was tested by linear regression using Δ clinical scores as dependent variable and HSPs levels and their variations over time (ΔHSP) as predictors. The level of statistical significance was set at $p<0.05$ for all tests.

3.3 Bioinformatics and ML algorithm for prognosticating patient's outcome

3.3.1 Model adaptation

Notably, AI require large and well-refined dataset in order to develop robust and generalizable predictive algorithms. Therefore, the development of a ML algorithm capable of prognosticate patient's outcome based on early clinical and radiological data demands a *wide and curated dataset*. Such dataset must include a large number of cases and high-quality features in order to ensure proper training, avoid overfitting and ensure reliable results across different patient subgroups.

According to this requirement, the small population of ET and PD patients enrolled of the first branch of the study represented a substantial limit for the development of a ML algorithm. Thus, this limit was exceeded by the adoption of a "mock" *reference scenario* for which a high number of cases was immediately available, with baseline radiological images and repeated blood test. Since the wide number of cases with such these features, traumatic brain injury (TBI) was used as mock reference scenario in order to develop a reliable ML algorithm which can be properly trained in a reproducible and generalizable way in place of tcMRgFUS thalamotomy and without the limit of that small sample size.

In particular, as mock features, brain CT scans of patients with TBI were used in place of brain MRI of ET and PD patients undergone tcMRgFUS thalamotomy; serum albumin of TBI patients was used as *assessment feature* in place of HSPs of ET and PD patients; Glasgow Outcome Score (GOS) and modified Rankin score (mRS) at discharge were used as *outcome indicators* or *targets* in place of neurological outcome and tremor improvement of ET and PD patients undergone tcMRgFUS thalamotomy.

3.3.2 Population

For the purpose of this branch of the study, a retrospective cohort study was performed at ARNAS Civico (Palermo – Italy) in order to collect clinical and radiological data. Hospital electronic registries were queried for patients admitted to the emergency room (ER) with admission diagnoses of TBI with the following ICD9-CM codes and child subcategories:

- 800 Fracture of skull vault,
- 801 Fracture of skull base,
- 803 Other and unqualified skull fractures,

- 804 Multiple fractures involving skull or face with other bones,
- 850 Concussion,
- 851 Cerebral laceration and contusion,
- 852 Subarachnoid, subdural, and extradural hemorrhage, following injury,
- 853 Other and unspecified intracranial hemorrhage following injury,
- 854 Intracranial injury of other and unspecified nature,
- 905.0 Late effect of fracture of skull and face bones,
- 907.0 Late effect of intracranial injury without mention of skull fracture

Among the whole population, inclusion criteria were: first brain CT scan after TBI performed on ER admission and retrievable CT scan from hospital archiving system, presence of thin slice sequences with 1.2-1.5mm thickness performed with brain windowing in helical acquisition and sufficient clinical data about patient's outcome at the time of hospital discharge classified with GOS and mRS; serum albumin on admission and repeated blood test during hospital stay. Exclusion criteria were lack of brain CT scan on ER admission, late follow up brain CT scan performed on ER admission, non-native series and post-processed brain CT scan, lack of clinical data about patient's outcome, lack of serum albumin on hospital admission, evidence of chronic subdural hematoma.

For each enrolled patient, brain CT scan performed at hospital admission was retrieved and demographics (sex, age at hospitalization), clinical data (serum albumin at admission, eventually repeated serum albumin, Glasgow coma scale ad admission, GOS and mRS at hospital discharge) were recorded

3.3.3 Radiomics pipeline and analysis from whole-brain segmentation

Brain CT scan of enrolled patient was properly post-processed in order to finally obtain radiomic data from patient's whole-brain segmentation. Brain CT scan segmentation was performed by the use of 3D Slicer, an open-source software coded in Python for medical image segmentation and advanced processing.

Whit 3D Slicer the post-processing pipeline was the following: first, the retrieved CT scan from hospital archiving system was stored into local DICOM database; then, thin-slice series (1.2-1.5mm) with brain window was loaded and underwent automatic *skull stripping* by the use of a standardized open source script (*Swiss Skull Stripper* - Skull-Stripper Filter for ITK by Stefan Bauer, Thomas Fejes and Mauricio Reyes, Institute for Surgical Technology and Biomechanics, University of Bern, Switzerland). Then, the brain volume (named "Brain_RAW") thus created was further refined by the use of Segmentation editor. In particular, brain volume was masked by *thresholding* (minimum value 0 HU, maximum value 100HU), in order to exclude remnants of bone-density voxels. Then, further refinement was performed by *island removal* (with the removal of islands less wider than 1000 voxel) and *smoothing* by closing (fill holes) algorithm with a kernel of 3x3x3 px.

At this point of the post-processing pipeline, a new mask (named "Brainmask_DEF") corresponding only to brain voxels including ventricles and arachnoid cisterns, without any bone, soft tissue or

element external to the neurocranium is created along with a new volume (named “Brain_DEF”) made by a DICOM series containing only patient’s brain, whose volume was isolated from brain CT scan upon “Brainmask_DEF”.

Then, radiomic analysis was performed by the use of PyRadiomics, an open-source library for the systematic and standardized extraction of quantitative features from medical images. From the analysis of medical images, it is capable of calculating a wide range of quantitative descriptors representing morphological, statistical, and textural characteristics from a defined Region of Interest (ROI) of medical images. Radiomics features in PyRadiomics are organized into seven main classes:

- *First-Order Statistics:*
  19 features which describe the statistical distribution of intensity values within the ROI, without considering the voxels spatial relationships, providing a synthetic representation of image intensity. They include Energy, Total Energy, Entropy, Minimum, Maximum, Mean, Median, Interquartile Range, Range, Mean Absolute Deviation (MAD), Robust Mean Absolute Deviation (rMAD), Root Mean Squared (RMS), Standard Deviation, Skewness, Kurtosis, Variance, Uniformity.
- *Shape-based Features (2D and 3D):*
  14 3D features and 10 2D features, which describe the geometry and morphology of the ROI. 3D measures include Mesh Volume, Voxel Volume, Surface Area, Surface Area to Volume ratio, Sphericity, Compactness 1, Compactness 2, Spherical Disproportion, Maximum 3D diameter, Maximum 2D diameter (Slice), Maximum 2D diameter (Column), Maximum 2D diameter (Row), Major Axis Length, Minor Axis Length, Least Axis Length, Elongation, Flatness. 2D measures include Mesh Surface, Pixel Surface, Perimeter, Perimeter to Surface ratio, Sphericity, Spherical Disproportion, Maximum 2D diameter, Major Axis Length, Minor Axis Length, Elongation.
- *GLCM – Gray Level Co-occurrence Matrix:*
  24 features which evaluate the frequency in which pairs of gray levels appear at a given distance and direction, describing image texture in terms of regularity, granularity, and local complexity. They include autocorrelation, Joint Average, Cluster Prominence, Cluster Shade, Cluster Tendency, Contrast, Correlation, Difference Average, Difference Entropy, Difference Variance, Joint Energy, Joint Entropy, Informational Measure of Correlation (IMC) 1, Informational Measure of Correlation (IMC) 2, Inverse Difference Moment (IDM), Maximal Correlation Coefficient (MCC), Inverse Difference Moment Normalized (IDMN), Inverse Difference (ID), Inverse Difference Normalized (IDN), Inverse Variance, Maximum Probability, Sum Average, Sum Entropy, Sum of Squares.
- *GLRLM – Gray Level Run Length Matrix:*
  16 features which consider the length of adjacent voxels with the same gray level in a specific direction evaluating texture linear coherence or fragmentation. They include Short Run

Emphasis (SRE), Long Run Emphasis (LRE), Gray Level Non-Uniformity (GLN), Gray Level Non-Uniformity Normalized (GLNN), Run Length Non-Uniformity (RLN), Run Length Non-Uniformity Normalized (RLNN), Run Percentage (RP), Gray Level Variance (GLV), Run Variance (RV), Run Entropy (RE), Low Gray Level Run Emphasis (LGLRE), High Gray Level Run Emphasis (HGLRE), Short Run Low Gray Level Emphasis (SRLGLE), Short Run High Gray Level Emphasis (SRHGLE), Long Run Low Gray Level Emphasis (LRLGLE), Long Run High Gray Level Emphasis (LRHGLE).

- *GLSZM – Gray Level Size Zone Matrix:*

  16 features which measures the homogeneity and size of homogeneous areas. They include Small Area Emphasis (SAE), Large Area Emphasis (LAE), Gray Level Non-Uniformity (GLN), Gray Level Non-Uniformity Normalized (GLNN), Size-Zone Non-Uniformity (SZN), Size-Zone Non-Uniformity Normalized (SZNN), Zone Percentage (ZP), Gray Level Variance (GLV), Zone Variance (ZV), Zone Entropy (ZE), Low Gray Level Zone Emphasis (LGLZE), High Gray Level Zone Emphasis (HGLZE), Small Area Low Gray Level Emphasis (SALGLE), Small Area High Gray Level Emphasis (SAHGLE), Large Area Low Gray Level Emphasis (LALGLE), Large Area High Gray Level Emphasis (LAHGLE).

- *NGTDM – Neighboring Gray Tone Difference Matrix:*

  5 features which considers the difference between a voxel's value and the average of its neighbors, providing a measure of local variation and spatial organization. They are coarseness, contrast, busyness, complexity, strength.

- *GLDM – Gray Level Dependence Matrix:*

  14 features which evaluate the number of dependent voxels with a given gray level relative to a central voxel, reflecting the size and uniformity of intensity dependencies: They are Small Dependence Emphasis (SDE), Large Dependence Emphasis (LDE), Gray Level Non-Uniformity (GLN), Dependence Non-Uniformity (DN), Dependence Non-Uniformity Normalized (DNN), Gray Level Variance (GLV), Dependence Variance (DV), Dependence Entropy (DE), Low Gray Level Emphasis (LGLE), High Gray Level Emphasis (HGLE), Small Dependence Low Gray Level Emphasis (SDLGLE), Small Dependence High Gray Level Emphasis (SDHGLE), Large Dependence Low Gray Level Emphasis (LDLGLE), Large Dependence High Gray Level Emphasis (LDHGLE).

For the purpose of this study radiomics analysis was performed using PyRadiomics module (a graphical user interface of PyRadiomics for 3D slicer) using “Brain_DEF” as input image and “Brainmask_DEF” as input regions: in this way radiomic analysis is performed for the whole brain volume, instead of single regions, in order to use 3D mask of the whole brain volume as a single ROI for radiomics features extrapolation. PyRadiomics was requested to analyze all radiomic features (*first order, second order, shape-based features, texture-related features, sequential features*) with verbose output saved in a .csv table named “Radiomics”.

At the end, this pipeline extrapolated 120 radiomic features from the whole brain segmentation and analyzed for each patient. [**Figure 1**]

Radiomic data of each patient were stored in a single dataset containing also demographic and clinical data for the training of and further analysis by ML algorithm.

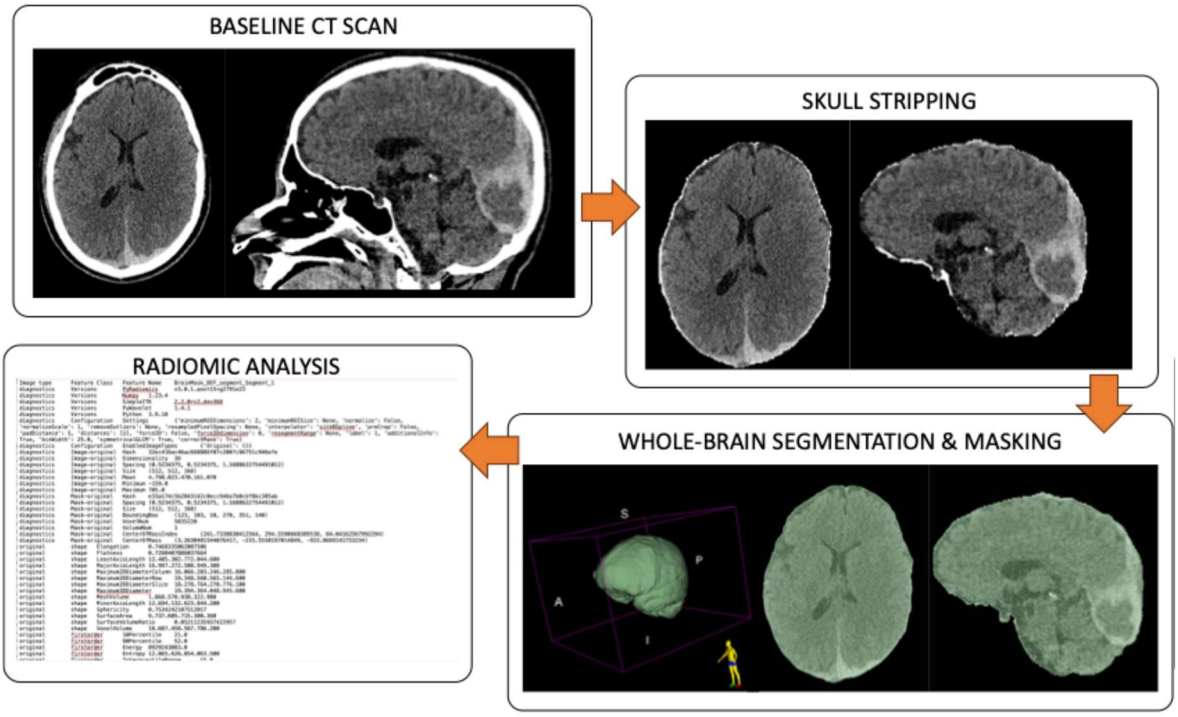

Figure 1 *Schematic pipeline of data extraction for radiomic analysis from brain CT scan, automated skull stripping and whole brain segmentation*

3.3.4 Development and training of supervised ML algorithm

For the purpose of this study, a **ML algorithm** was programmed using Python (version 3.10) as opensource programming language under PyCharm. The analysis was designed to implement an automated classification pipeline based on Random Forest Classifier applied to radiomic data. This ML algorithm was coded by the use of several open-source libraries (*Pandas, Numpy, Scikit-learn, matplotlib, Seaborn*), which are highly established and widely used for scientific purposes. The script was coded in order to elaborate the entire analytic flow, from data loading to the evaluation of predictive performance of the algorithm.

In particular, radiomic data are imported from .csv dataset using a dedicated function, which verifies the file compatibility and returns a Pandas Dataframe suitable for further processing. Then, during a pre-processing phase any missing value and any non-informative or redundant columns are removed;

categorical variables, if present, are converted in order to ensure the quality and reliability of the input data.

Then, numerical features are standardized through a z-score transformation (mean 0, standard deviation 1), using the StandardScaler class from the scikit-learn library. Normalization is a critical step for further dimensionality reduction by Principal Component Analysis (PCA). PCA is used to synthesize the information contained in a large number of radiomics variables into a small number of uncorrelated principal components, preserving most of the dataset's informative variance. For the purpose of this study and the development of a ML algorithm for radiomic analysis, PCA is usefully adopted because the number of features exceeds the number of observations.

After the application of dimensionality reduction, the dataset thus reduced is split into a training set and a test set according to a predefined ratio (70 training : 30 test) using the train_test_split function. This split allows the model to be trained on a subset of the data and tested on previously unseen data, ensuring a more realistic assessment of the model's generalizability.

Because of the presence of multiple independent variables (120 radiomic features and serum albumin), Random Forest Classifier was used for classification, since its robustness even in presence of non-linear features. The classifier is trained on the principal components obtained from PCA and then applied to the test set in order to predict patient’s outcome.

The model performance is evaluated using confusion matrix, classification report (including accuracy, precision, sensitivity, specificity, and F1 score), and ROC/AUC analysis. ROC curves and their corresponding areas under the curve (AUC) are generated to assess model reliability. At the end several multidimensional diagrams are generated in order to facilitate the interpretation of the results.

The primary objective of this pipeline is to build a predictive model for classification of clinical outcome of neurosurgical patients based on baseline radiomics data. Looking forward, this model could be generically extended to other clinical scenarios where radiological and clinical /molecular information can be integrated in order to prognosticate patient’s prognosis (such as after tcMRgFUS thalamotomy by the integration of radiomic data from post-operative MRI and serum HSPs) and to develop personalized decision-making tools for precision medicine.

4 Results

4.1 HSPs expression in tcMRgFUS thalamotomy for tremor

Among the 27 patients underwent tcMRgFUS thalamotomy for refractory tremor at Unit of Neurosurgery – University of Palermo, only 14 patients completed the minimal required follow up with clinical evaluation ad blood sampling at T0-T1-T2 and were included in the study (7 PD patients and 7 ET patients, mean age 67.9 years, 12 Male and 2 Female). All of 14 enrolled patients underwent left VIM thalamotomy for predominant right limbs tremor.

For subgroup analysis, among ET patients (5 males and 2 females, mean age 67.29 years, min 49 - max 92) the pre-operative CRST score was 47.14 (min 20 max 78) and pre-operative CRST-Hand sub score was 10.89 (min 4 max 16); at T1 CRST score was 15.57 (min 4 – max 36) and CRST-Hand sub score was 1.71 (min 0 – max 5); at T2 CRST score was 25.57 (min 11 – max 41) and CRST-Hand sub score was 6.57 (min 1 - max 13). **[Table 1, Figure 2]**

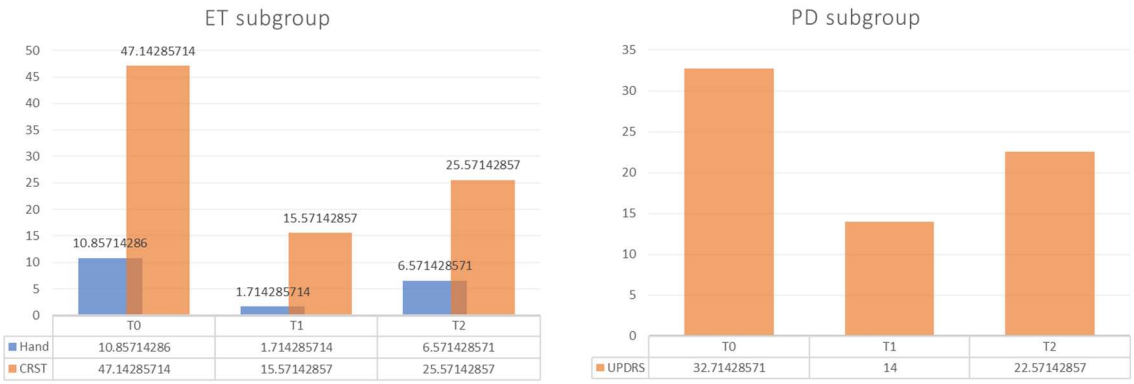

Figure 2 *Overview of mean clinical score of ET and PD patients measured before surgery (T0), 48h after surgery (T1) and 1 month after surgery (T2)*

In parallel, plasma levels of HSP27, HSP40, and HSP90 were assessed at the three time points (T0, T1, and T2) in all enrolled patients. Among the analyzed heat shock proteins, only HSP90 showed a statistically significant variation in plasma concentration following the treatment, as further described, suggesting a potential association with the therapeutic effect of tcMRgFUS thalamotomy **[Figure 3]**. On the other hand, HSP27 showed very low values below the sensitivity of ELISA immunoassay, resulting in negative values of serum concentration; thus, HSP27 was excluded from further analysis since it cannot be used as clinical marker.

After excluding HSP27 from statistical analysis, numerical variables were globally tested for normality with Shapiro-Wilk test ad most of them showed a non-normal distribution ($p>0.05$). **[Table 2]**

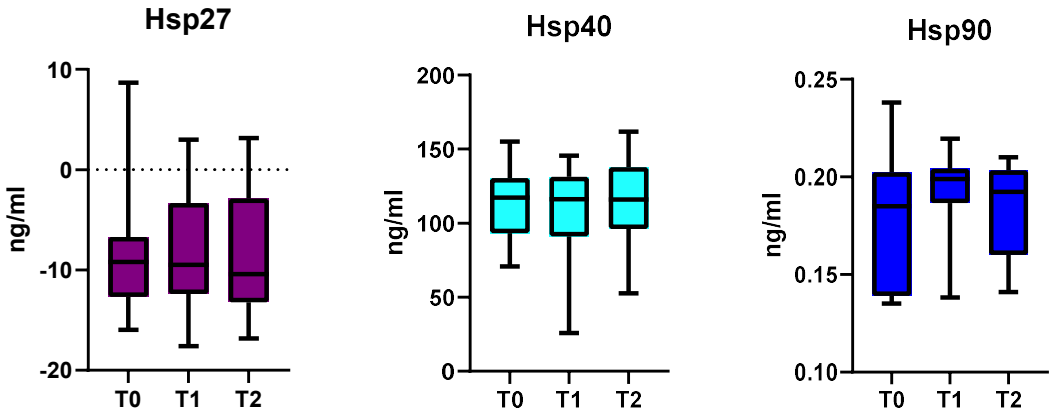

Figure 3. Plasma levels of HSP27, HSP40, and HSP90 in patients undergoing tcMRgFUS thalamotomy. *Box plots show the distribution of plasma concentrations (ng/ml) of HSP27 (left, purple), HSP40 (center, cyan), and HSP90 (right, blue) at three time points: T0 (pre-operative), T1 (48 hours post-operative), and T2 (1-month post-operative). No significant changes were observed in HSP27 and HSP40 levels across time points. In contrast, HSP90 levels showed a statistically significant increase at T1 compared to T0 ($p = 0.038$) suggesting a potential early stress-related response following treatment.*

ID	PATH	AGE	T0 HAND	T1 HAND	T2 HAND	T0 CRST	T1 CRST	T2 CRST	T0 UPDRS	T1 UPDRS	T2 UPDRS	HSP90 T0	HSP90 T1	HSP90 T2	HSP27 T0	HSP27 T1	HSP27 T2	HSP40 T0	HSP40 T1	HSP40-T2
1	ET	77	16	4	5	78	36	41				0.135105	0.149296	0.143808	8.682927	3	3.170732	124.342	145.6632	141.4404
2	ET	60	9	1	3	49	15	28				0.169446	0.171441	0.16551	-6.14634	-2.7561	-3.4878	90.68912	90.19689	52.81347
3	ET	64	4	0	1	27	10	12				0.136574	0.138237	0.141064	-13.6585	-14.7561	-14.2927	149.9896	123.1762	144.9637
4	ET	49	9	0	11	36	14	31				0.139374	0.218559	0.142339	-8.36585	-1.68293	-10.9268	127.1658	133.2539	115.715
5	ET	50	11	2	7	54	8	16				0.138293	0.198215	0.17765	-9.26829	-8.14634	-7.63415	133.6684	116.0259	117.8912
6	ET	92	16	5	13	66	22	40				0.199407	0.199795	0.200405	-9.09756	-8.82927	-9.82927	70.81865	102.2176	110.6632
7	ET	79	11	0	6	20	4	11				0.188625	0.192755	0.196109	-15.9512	-12.1463	-13.7561	83.64249	74.13472	83.82383
8	PD	57							38	18	16	0.197966	0.200322	0.193947	1.414634	-3.5122	2.439024	155.0415	144.3679	161.829
9	PD	77							41	24	59	0.181197	0.205116	0.20883	-12.0976	-11.9268	-1.02439	94.93782	97.42487	1.699482
10	PD	74							45	12	10	0.238099	0.219612	0.210022	-6.87805	-8.95122	-11.2927	117.4249	116.5959	116.0518
11	PD	66							47	16	5	0.210798	0.196829	0.190759	-12.0244	-10.4146	-11.5366	120.6632	125.6373	121.6995
12	PD	59							28	14	54	0.193947	0.203925	0.207195	-12.3171	-13.0976	-7.82927	113.6425	94.31606	134.0311
13	PD	70							14	10	10	0.169834	0.191646	0.183858	-14.8537	-17.5854	-16.8049	95.97409	26	69.05699
14	PD	76							16	4	4	0.215815	0.199573	0.202012	-8.12195	-9.95122	-13.0244	112.943	/	108.5648

***Table 1**: Clinical data and HSPs concentration of general population of ET and PD patients*

Descriptives

	Hand_T0	Hand_T1	Hand_T2	CRST_T0	CRST_T1	CRST_T2	UPDRS_T0	UPDRS_T1	UPDRS_T2	HSP90_T0	HSP90_T1	HSP90_T2	HSP40_T0	HSP40_T1	HSP40_T2
N	7	7	7	7	7	7	7	7	7	14	14	14	14	13	14
Mean	10.9	1.71	6.57	47.1	15.6	25.6	32.7	14.0	22.6	0.180	0.192	0.183	114	107	106
Median	11	1	6	49	14	28	38	14	10	0.185	0.199	0.192	116	116	116
Standard deviation	4.22	2.06	4.24	20.9	10.7	12.7	13.6	6.32	23.6	0.0329	0.0235	0.0252	24.4	32.4	41.9
Minimum	4	0	1	20	4	11	14	4	4	0.135	0.138	0.141	70.8	26.0	1.70
Maximum	16	5	13	78	36	41	47	24	59	0.238	0.220	0.210	155	146	162
Shapiro-Wilk W	0.914	0.836	0.963	0.972	0.906	0.885	0.881	0.995	0.750	0.931	0.836	0.856	0.976	0.908	0.903
Shapiro-Wilk p	0.422	0.091	0.842	0.909	0.368	0.249	0.232	0.999	**0.013***	0.314	**0.014***	0.027	0.942	0.174	0.125

***Table 2: S**ummary of clinical and serological variables analyzed for the whole population or ET and PD patients and tested for normality. Among 15 continues variables, only UPDRS_T2 and HSP90_T1 showed a normal distribution, thus non-parametric tests were used for further statistical analysis.*

HSP90 and HSP40 over time

Variation of **HSP90** serum level was non statistically significative when assessed globally for ET and PD patients over time (T0-T1-T2) (p=0.109) using Friedman's test as non-parametric analysis for paired data. However, a significative increase was observed only within the early post-operative period (T0 vs T1; **p=0.038**) suggesting a potential early stress-related response following the treatment **[Table 4].**

When analysis in restricted only to ET subgroup, HSP90 showed an overall significant variation over time (**p=0.018**), with a significant and persistent increase of HSP90 serum level both in the immediate post-operative course (T0 vs T1, **p=0.003**) and in long term follow up (T0 vs T2**, p=0.011**), supporting a sustained response and after treatment and an involvement of HSP90 in ET pathophysiology to be further investigated **[Table 5]**. On the other hand, no significant variation of HSP90 over time was found limited to PD subgroup (p=0.867). **[Table 6]**

As regards **HSP40**, no significant variation was shown both in global (p=0.735) and in subgroup analysis **[Tables 7-9]**

HSP90 vs HSP40

Subsequently, no correlation was found between expression of HSP90 and HSP40 over time (p>0.05) in the whole population of ET and PD patients **[Table 3]**. However, limited to ET subgroup, a correlation was found between HSP40 and HSP90 expression from pre-operative time to long-term follow up; in particular, HSP40 serum levels were negatively correlated to baseline HSP90 level over time (T1 $\rho = -0.786$, p = **0.048***; T1 $\rho = -0.786$, p = **0.048***; T2 $\rho = -0.821$, p = **0.034***), and only a positive correlation was found between late variation of HSP40 and HSP90 during long-term follow up (ΔT2-T1 $\rho = 0.786$ p = **0.048***. suggesting a possible mutual regulation or a divergent cellular response after surgery despite no significant overall variation of HSP40 was found during time. **[Suppl. 1]**

		HSP90_T0	HSP90_T1	HSP90_T2
HSP40_T0	**Spearman's rho**	-0.310	-0.002	-0.455
	p-value	0.281	1.000	0.104
HSP40_T1	**Spearman's rho**	-0.126	0.093	-0.341
	p-value	0.683	0.765	0.255
HSP40_T2	**Spearman's rho**	-0.112	-0.086	-0.279
	p-value	0.704	0.773	0.333

Table 3 *Spearman's correlation for HSP90 and HSP40 over time in ET and PD population. No correlation was found between HSP90 and HSP40 (p>0.05) suggesting different and non-correlated involvement of both HSPs in ET and PD*

Regarding clinical outcome, tcMRgFUS thalamotomy effectiveness was assessed separately for ET and PD subgroup by analysis of CRST score and CRST-Hand subscore for ET patients and UPDRS for PD patients.

A significant variation was shown both for CRST (**p<0.001***) and CRST-Hand subscore in ET patients (**p=0.002***) further confirmed by post-hoc analysis for paired data (T0 vs T1, T0 vs T2, T1 vs T2; **p<0.005***), suggesting a progressive and sustained improvement of tremor and hand fine motor performances over time after tcMRgFUS thalamotomy. **[Tables 10-11, Suppl. 2]**

In PD subgroup, UPDRS variation over time did not reach statistical significance (p=0.054), despite post-hoc analysis showed a significant reduction of UPDRS score from baseline to early post-operative phase (T0 vs T1, **p=0.02***) and late follow up (T0 vs T2, **p=0.036***), suggesting an early post-operative improvement which was sustained over time without any substantial modifications as confirmed by further correlation analysis (dUPDRS_T2-T1 vs dUPDRS_T2_T0 ρ= 0.9, p **<.001***). **[Table 12, Suppl. 3]**

HSP90 in whole ET and PD population

χ^2	df	p
4.43	2	0.109

Pairwise Comparisons (Durbin-Conover)

			Statistic	p
HSP90_T0	-	**HSP90_T1**	2.183	**0.038***
HSP90_T0	-	**HSP90_T2**	1.389	0.177
HSP90_T1	-	**HSP90_T2**	0.794	0.434

Table 4 *Non-parametric analysis for HSP90 variation over time in the whole population of enrolled ET and PD patients. Globally assessed in the whole population, HSP90 showed a significant variation only within the early post-operative period (T0 – T1).*

HSP90 in ET subgroup

χ^2	df	p
8.00	2	**0.018***

Pairwise Comparisons (Durbin-Conover)

			Statistic	p
HSP90_T0	-	**HSP90_T1**	3.780	**0.003***
HSP90_T0	-	**HSP90_T2**	3.024	**0.011***
HSP90_T1	-	**HSP90_T2**	0.756	0.464

Table 5 *Non-parametric analysis for HSP90 variation over time in the subgroup of enrolled ET patients. HSP90 showed a significant variation within the early post-operative period (T0 – T1) and in the long-term follow up (T0 – T2)*

HSP90 in PD subgroup

χ^2	df	p
0.286	2	0.867

Pairwise Comparisons (Durbin-Conover)

			Statistic	p
HSP90_T0	-	**HSP90_T1**	0.250	0.807
HSP90_T0	-	**HSP90_T2**	0.250	0.807
HSP90_T1	-	**HSP90_T2**	0.500	0.626

Table 6 *Non-parametric analysis for HSP90 variation over time in the subgroup of enrolled PD patients. No significant variation of HSP90 was shown over time*

HSP40 in whole ET and PD population

χ^2	df	p
0.615	2	0.735

Pairwise Comparisons (Durbin-Conover)

			Statistic	p
HSP40_T0	-	**HSP40_T1**	0.763	0.453
HSP40_T0	-	**HSP40_T2**	0.381	0.706
HSP40_T1	-	**HSP40_T2**	0.381	0.706

Table 7 *Non-parametric analysis for HSP40 variation over time in the whole population of enrolled ET and PD patients.*

HSP40 in ET subgroup

χ^2	df	p
0.286	2	0.867

Pairwise Comparisons (Durbin-Conover)

			Statistic	p
HSP40_T0	-	**HSP40_T1**	0.500	0.626
HSP40_T0	-	**HSP40_T2**	0.250	0.807
HSP40_T1	-	**HSP40_T2**	0.250	0.807

Table 8 *Non-parametric analysis for HSP40 variation over time in the subgroup of enrolled ET patients*

HSP40 in PD subgroup

χ^2	df	p
0.333	2	0.846

Pairwise Comparisons (Durbin-Conover)

			Statistic	p
HSP40_T0	-	**HSP40_T1**	0.535	0.605
HSP40_T0	-	**HSP40_T2**	0.267	0.795
HSP40_T1	-	**HSP40_T2**	0.267	0.795

Table 9 *Non-parametric analysis for HSP40 variation over time in the subgroup of enrolled PD patients.*

CRST score in ET subgroup

χ^2	df	p
14.0	2	**<.001***

Pairwise Comparisons (Durbin-Conover)

			Statistic	p
CRST_T0	-	**CRST _T1**	Inf	**<.001***
CRST _T0	-	**CRST _T2**	Inf	**<.001***
CRST _T1	-	**CRST _T2**	Inf	**<.001***

Table 10 *Non-parametric analysis for CRST score variation over time in the subgroup of enrolled ET patients, showing a significant and persistent reduction of global tremor after tcMRgFUS thalamotomy*

CRST-Hand subscore in ET subgroup

χ^2	df	p
12.3	2	**0.002***

Pairwise Comparisons (Durbin-Conover)

			Statistic	p
Hand_T0	-	**Hand _T1**	9.19	**<.001***
Hand _T0	-	**Hand _T2**	3.54	**0.004***
Hand _T1	-	**Hand _T2**	5.66	**<.001***

Table 11 *Non-parametric analysis for CRST-Hand subscore variation over time in the subgroup of enrolled ET patients, showing a significant and persistent reduction of contralateral hand tremor after tcMRgFUS thalamotomy*

UPDRS score in PD subgroup

χ^2	df	p
5.85	2	0.054

Pairwise Comparisons (Durbin-Conover)

			Statistic	p
UPDRS_T0	-	**UPDRS _T1**	2.692	**0.020***
UPDRS _T0	-	**UPDRS _T2**	2.355	**0.036***
UPDRS _T1	-	**UPDRS _T2**	0.336	0.742

Table 12 *Non-parametric analysis for UPDRS score variation over time in the subgroup of enrolled PD patients, showing a significant reduction of tremor after tcMRgFUS thalamotomy.*

HSPs and variation (ΔHSPs) over time

As regard correlation between HSPs serum levels and their variation over time (ΔHSP) after tcMRgFUS in the whole population of ET and PD patients, Spearman's correlation showed a significant stability of HSP90 and HSP40 expression over time.

In particular, **HSP90** expression during long-term follow up (T2) in general population is significantly correlated to pre-operative and early post-operative serum levels (T0 ρ=0.793, p=**0.001***; T1; ρ=0.640, p=**0.016***). Similarly, **HSP40** showed a persistent expression from the pre-operative period to the early and late post-operative follow up (T0-T1 ρ =0.742 p=**0.005***; T0-T2 ρ=0.802, p<**0.001***; T1-T2 ρ=0.714, p=**0.008***), suggesting the lack of a significant influence of tcMRgFUS thalamotomy on HSP40 expression.

Analysis of **HSPs variations** over time (ΔHSP) in general population showed significant relationships with absolute HSPs values: in particular, high baseline HSP90 expression is associated with lower increases during long-term follow-up (ΔT2–T0; ρ= -0.657, p = **0.013***), suggesting a possible *ceiling effect*. Furthermore, early post-operative HSP90 variation (T1–T0) is strongly associated with late change (T2–T0; ρ = 0.820, p < **0.001***), suggesting a *predictable trend* over time. As regards HSP40, a substantial longitudinal balance was found over time, with a negative correlation between early post-operative HSP40 level and late variation during long-term follow up (ρ=–0.725, p=**0.007***), confirming the lack of significant influence on its expression by tcMRgFUS thalamotomy. **[Suppl. 1]**

Refining the analysis for pathology, in **ET subgroup** no significant intrinsic correlation was found within HSPs serum levels over time after tcMRgFUS thalamotomy, suggesting that post-operative HSPs expression is not influenced by pre-operative serum levels. **[Suppl. 2]**

In **PD subgroup**, a strong positive correlation was shown between early post-operative and late follow up HSP90 levels (T1 – T2 ρ = 0.964, p = **0.003*),** suggesting a substantial expression during follow up; however, high baseline expression of HSP90 is related to lower increase during early post-operative period and late follow up (ΔHSP90_T1_T0 ρ = -0.964, p = **0.003*;** ΔHSP90_T2_T0 ρ = –0.929, p **= 0.007***) supporting the hypothesis of a *ceiling effect* in PD patients. As regards HSP40, expression during late follow up is strongly related to its baseline expression (T0 – T2 ρ = 0.893, p = **0.012***), and high baseline expression is related to higher cumulative increase during late follow up (ΔHSP40_T2_T0 ρ = 0.786, p = **0.048***) suggesting the lack of tcMRgFUS influence on HSP40 expression **[Suppl. 3]**

Clinical effectiveness vs HSPs

For the evaluation of clinical effectiveness of tcMRgFUS thalamotomy, positive variations of clinical scores (ΔHand, ΔCRST, ΔUPDRS > 0) were considered as *tremor worsening* between two time points since the higher the score is the worse the tremor is both for ET and PD patients.

Correlation between HSPs expression and clinical effect on tremor was separately evaluated for ET and PD subgroup. In **ET patients**, no significant correlation was found between clinical outcome and absolute HSP90 serum levels during time. However, higher post-operative HSP90 levels are strongly related to clinical

worsening after a good post-operative response both on hand motor function and global tremor rate on long-tremor follow up (ΔHand_T2_T1; ρ = 0.955, p **< 0.001***; ΔCRST_T2_T1; ρ = 0.857, p = **0.024***). Moreover, the worsening of hand tremor is synchronous to the worsening of global tremor (ΔCRST_T2_T1 vs ΔHand_T2_T1; ρ = 0.811, p = **0.027***) during late follow up and the overall effect on tremor proportional to the overall post-operative improvement (ΔCRST_T2_T0 vs ΔCRST_T1_T0; ρ = 0.857, p = **0.024***), suggesting the hypothesis that HSP90 represents an early negative biological marker of late clinical worsening of tremor in ET patients undergone tcMRgFUS thalamotomy. **[Suppl. 2]**

In **PD patients** a significant correlation was shown between cumulative HSP90 increase during late follow up and the worsening of overall motor performance (ΔHSP90_T2_T0 vs ΔUPDRS_T2_T0; ρ = 0.821, p = **0.034***), suggesting the abovementioned hypothesis of a negative prognostic value of HSP90 even in PD patients. **[Suppl. 3]**

Significant correlations between clinical scores and HSPs levels from Spearman's test were further analyzed by univariate linear regression in order to assess association between tremor worsening during late follow up and HSPs expression. Subsequently, significant predictors were further analyzed in multivariate logistic regression with absolute HSPs serum levels and ΔHSPs for both ET and PD subgroups.

In **ET subgroups**, since the significant improvement of tremor after tcMRgFUS thalamotomy, univariate linear regression showed that early post-operative HSP90 expression represents a strong predictor of tremor worsening from early to late post-operative follow up (ΔHand_T2_T1 vs HSP90_T1 $R^2 = 0.864$, $F(1,5) = 31.9$, p = **0.002***), with a reliable estimation of tremor worsening (β = 121.1 ± 21.44, p = **0.002***) and late estimated improvement only in case of no early post-operative increase of HSP90 expression (intercept –17.1 ± 3.93, p = **0.007***) **[Table 13, Figure 4].**

Consistently, higher post-operative HSP90 expression is significantly associated to a worsening of overall tremor during late follow up after early post-operative improvement (ΔCRST_T2_T1 vs HSP90_T1 $R^2 = 0.580$, p = 0.047*) with a reliable estimation and significant tremor worsening in case of HSP90 increase after tcMRgFUS thalamotomy (β = 159.2 ± 60.6, p = **0.047***) **[Table 14, Figure 5]**. However, the worsening of overall tremor assessed by CRTS is not confirmed in multivariate analyses considering HSP90 levels and their variations over time ($R^2 = 0.792$, p = 0.151) **[Tables 17-18]**

Multivariate linear regression confirmed the influence of HSP90 on hand tremor worsening during late follow up after post-operative good clinical response ($R^2 = 0.915$, p = **0.041***). However, only early post-operative HSP90 expression contributes significantly to the late clinical worsening of hand tremor (HSP90_T1 β = 134.0, p = **0.013***) [**Table 15]**. Additionally, variation of HSP90 levels during early (ΔHSP90_T1_T0) and late post-operative period (ΔHSP90_T2_T1) showed no significant effect both on hand tremor and overall tremor during long-term follow up after post-operative improvement (ΔHand_T2_T1 $R^2 = 0.459$, $F(2,4) = 1.70$, p = 0.293; ΔCRST_T2_T1 $R^2 = 0.359$, $F(2,4) = 1.12$, p = 0.410) [**Table 16].**

Linear Regression dHand_T2_T1 vs HSP90_T1

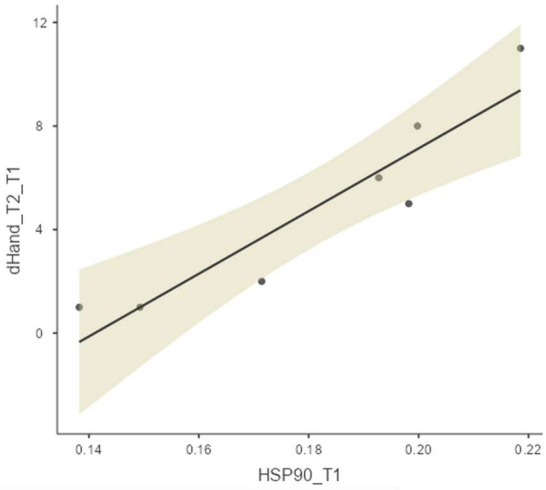

Model Fit Measures

			Overall Model Test			
Model	**R**	**R^2**	**F**	**df1**	**df2**	**p**
1	0.930	0.864	31.9	1	5	**0.002***

Model Coefficients – dHand_T2_T1

			95% CI					95% CI	
Predictor	**Estimate**	**SE**	**Lower**	**Upper**	**t**	**p**	**SE**	**Lower**	**Upper**
Intercept	-17.1	3.93	-27.2	-6.98	-4.35	**0.007***			
HSP90_T1	121.1	21.44	65.9	176.17	5.65	**0.002***	0.930	0.506	1.35

Table 13, Figure 4 *Linear regression analysis of Hand tremor variation between early and late post-operative period and post-operative expression of HSP90, showing a significant and predictable worsening of hand tremor related to post-operative HSP90 expression.*

Linear Regression dCRST_T2_T1 vs HSP90_T1

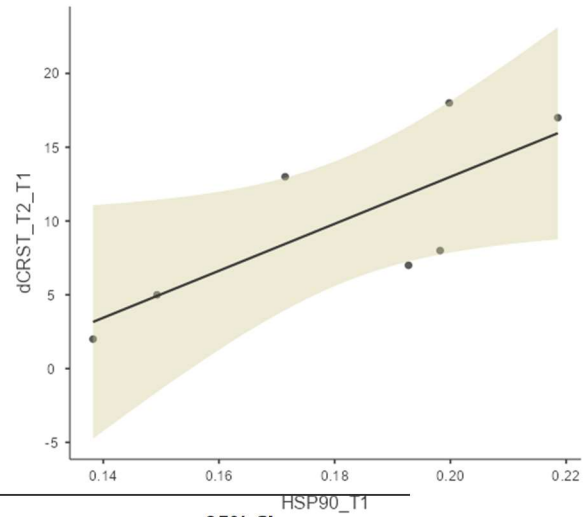

Model Fit Measures

			Overall Model Test			
Model	**R**	**R^2**	**F**	**df1**	**df2**	**p**
1	0.761	0.580	6.89	1	5	**0.047***

Note. Models estimated using sample size of N=7

Model Coefficients - dCRST_T2_T1

			95% CI					95% CI	
Predictor	**Estimate**	**SE**	**Lower**	**Upper**	**t**	**p**	**SE**	**Lower**	**Upper**
Intercept	-18.8	11.1	-47.40	9.71	-1.70	0.151			
HSP90_T1	159.2	60.6	3.31	315.05	2.63	**0.047***	0.761	0.0158	1.51

Table 14, Figure 5 *Linear regression analysis of overall tremor (CRST) variation between early and late post-operative period and post-operative expression of HSP90, showing a significant and predictable worsening of tremor related to post-operative HSP90 expression.*

Linear Regression dHand_T2-T1 vs HSP90s

Model Fit Measures

			Overall Model Test			
Model	**R**	**R^2**	**F**	**df1**	**df2**	**p**
1	0.956	0.915	10.7	3	3	**0.041***

Note. Models estimated using sample size of N=7

Model Coefficients - dHand_T2_T1

			95% CI					95% CI	
Predictor	**Estimate**	**SE**	**Lower**	**Upper**	**t**	**p**	**SE**	**Lower**	**Upper**
Intercept	-15.5	4.84	-30.9	-0.0462	-3.19	0.050			
HSP90_T0	48.3	46.05	-98.2	194.9055	1.05	0.371	0.348	-0.707	1.403
HSP90_T1	134.0	25.07	54.2	213.7833	5.35	**0.013***	1.029	0.416	1.642
HSP90_T2	-69.6	52.64	-237.1	97.9275	-1.32	0.278	-0.466	-1.588	0.656

Table 15 *Linear regression analysis of Hand tremor variation between early and late post-operative period and expression of HSP90 during pre and post-operative time. Despite an overall significance of HSP90 levels, only early post-operative expression of HSP90 contributes to Hand tremor worsening from early to late post-operative period*

Linear Regression dCRST_T2-T1 vs HSP90s

Model Fit Measures

			Overall Model Test			
Model	**R**	**R^2**	**F**	**df1**	**df2**	**p**
1	0.890	0.792	3.80	3	3	0.151

Note. Models estimated using sample size of N=7

Model Coefficients - dCRST_T2_T1

			95% CI					95% CI	
Predictor	**Estimate**	**SE**	**Lower**	**Upper**	**t**	**p**	**SE**	**Lower**	**Upper**
Intercept	-20.2	12.1	-58.9	18.4	-1.67	0.194			
HSP90_T0	201.5	115.4	-165.9	568.9	1.75	0.179	0.903	-0.744	2.550
HSP90_T1	177.5	62.8	-22.5	377.5	2.82	0.067	0.849	-0.108	1.805
HSP90_T2	-202.6	132.0	-622.5	217.4	-1.53	0.222	-0.845	-2.597	0.907

Table 17 *Linear regression analysis of overall tremor variation between early and late post-operative period and expression of HSP90 during pre and post-operative time.*

Linear Regression dHand_T2-T1 vs dHSP90s

Model Fit Measures

			Overall Model Test			
Model	**R**	**R^2**	**F**	**df1**	**df2**	**p**
1	0.677	0.459	1.70	2	4	0.293

Note. Models estimated using sample size of N=7

Model Coefficients - dHand_T2_T1

			95% CI					95% CI	
Predictor	**Estimate**	**SE**	**Lower**	**Upper**	**t**	**p**	**SE**	**Lower**	**Upper**
Intercept	3.67	1.68	-1.00	8.34	2.180	0.095			
dHSP90_T1_T0	-14.75	98.69	-288.76	259.26	-0.149	0.888	-0.126	-2.47	2.22
dHSP90_T2_T1	-105.59	113.05	-419.48	208.29	-0.934	0.403	-0.789	-3.13	1.56

Table 16 *Linear regression analysis of Hand tremor variation between early and late post-operative period and variation of HSP90 levelsduring pre and post-operative time.*

Linear Regression dCRST_T2-T1 vs dHSP90s

Model Fit Measures

			Overall Model Test			
Model	**R**	**R^2**	**F**	**df1**	**df2**	**p**
1	0.600	0.359	1.12	2	4	0.410

Note. Models estimated using sample size of N=7

Model Coefficients - dCRST_T2_T1

			95% CI					95% CI	
Predictor	**Estimate**	**SE**	**Lower**	**Upper**	**t**	**p**	**SE**	**Lower**	**Upper**
Intercept	9.68	2.94	1.52	17.8	3.294	0.030			
dHSP90_T1_T0	-148.91	172.46	-627.73	329.9	-0.863	0.437	-0.794	-3.35	1.76
dHSP90_T2_T1	-258.87	197.55	-807.36	289.6	-1.310	0.260	-1.204	-3.76	1.35

Table 18 *Linear regression analysis of overall tremor variation between early and late post-operative period and variation of HSP90 levels during pre and post-operative time*

In PD subgroup, univariate linear regression showed that cumulative variation of post-operative HSP90 expression represents a significant predictor of overall tremor worsening after an early post-operative improvement (ΔUPDRS_T2_T0 vs ΔHSP90_T2_T0 $R^2 = 0.770$, $F(1,5) = 16.7$, p = **0.009***), with a reliable estimation of tremor worsening (β = 1094.96 ± 267.67, p = **0.009***), confirmed the former correlation evidenced by Spearman test and suggesting that cumulative increase of HSP90 serum level during follow up is associated with a worsening of overall tremor in PD patients. **[Table 19, Figure 6]**

Despite no correlation was found with Spearman test, multivariate regression with early (ΔHSP90_T1−T0) and late (ΔHSP90_T2_T1) post-operative HSP90 serum level - in order to avoid collinearity error with ΔHSP90_T2_T0, showed a significant correlation with late cumulative clinical outcome (R = 0,941; R^2 = 0,886; F(2,4) = 15,6; p = **0,013***), predicting tremor worsening with the increasing expression of HSP90 both during the early (ΔHSP90-T1_T0 β = 818 ± 251; p = **0,031***) and in the late post-operative period (ΔHSP90_T2_T1 β = 2612 ± 780; p = **0,029***) **[Table 20]**.

Moreover, significant relationship was found between cumulative motor outcome during late follow up (ΔUPDRS_T2−T0) and HSP90 expression over time ($R^2 = 0.912$, $F(3,3) = 10.3$, p = **0.043***); in particular, HSP90 baseline expression is negatively correlated (β = −912 SE = 274, p = **0.045***) and HSP90 expression during late follow up is positively correlated to late cumulative motor worsening (β = 2589, SE = 792, p = **0.047***) suggesting that higher pre-operative HSP90 expression is correlated to lower odd of tremor worsening during late follow up and confirming that higher late post-operative expression in predictive of clinical worsening during late follow up even in PD patients **[Table 21]**.

Linear Regression dUPDRS_T2_T0 vs dHSP90_T2_T0

Model Fit Measures

			Overall Model Test			
Model	**R**	**R^2**	**F**	**df1**	**df2**	**p**
1	0.877	0.770	16.7	1	5	0.009

Note. Models estimated using sample size of N=7

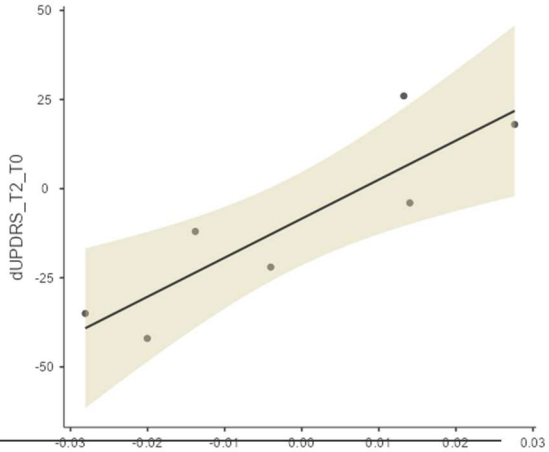

Model Coefficients - dUPDRS_T2_T0

			95% CI					95% CI	
Predictor	**Estimate**	**SE**	**Lower**	**Upper**	**t**	**p**	**SE**	**Lower**	**Upper**
Intercept	-8.42	5.09	-21.5	4.67	-1.65	0.159			
dHSP90_T2_T0	1094.36	267.67	406.3	1782.43	4.09	0.009	0.877	0.326	1.43

Table 19, Figure 6 *Linear regression analysis of overall tremor (UPDRS) variation and variation of HSP90 levels between pre-operative and late post-operative period, showing a significant and predictable worsening of tremor related to post-operative variation of HSP90 expression.*

Linear Regression dUPDRS_T2_T0 vs dHSP90s

Model Fit Measures

			Overall Model Test			
Model	**R**	**R^2**	**F**	**df1**	**df2**	**p**
1	0.941	0.886	15.6	2	4	**0.013***

Note. Models estimated using sample size of N=7

Model Coefficients - dUPDRS_T2_T0

			95% CI					95% CI	
Predictor	**Estimate**	**SE**	**Lower**	**Upper**	**t**	**p**	**SE**	**Lower**	**Upper**
Intercept	-3.63	4.65	-16.5	9.29	-0.779	0.479			
dHSP90_T1_T0	817.98	251.02	121.0	1514.93	3.259	**0.031***	0.576	0.0852	1.07
dHSP90_T2_T1	2612.08	779.91	446.7	4777.47	3.349	**0.029***	0.592	0.1013	1.08

Table 20 *Linear regression analysis of overall tremor (UPDRS) variation and variation of HSP90 levels between pre-operative and late post-operative period. Both early and late post-operative variation of HSP90 levels contribute to overall cumulative tremor worsening.*

Linear Regression dUPDRS_T2_T0 vs HSP90s

Model Fit Measures

			Overall Model Test			
Model	**R**	**R^2**	**F**	**df1**	**df2**	**p**
1	0.955	0.912	10.3	3	3	**0.043***

Note. Models estimated using sample size of N=7

Model Coefficients - dUPDRS_T2_T0

			95% CI					95% CI	
Predictor	**Estimate**	**SE**	**Lower**	**Upper**	**t**	**p**	**SE**	**Lower**	**Upper**
Intercept	-106	109	-451.9	240.8	-0.970	0.404			
HSP90_T0	-912	274	-1783.5	-40.3	-3.329	**0.045***	-0.814	-1.5911	-0.0359
HSP90_T1	-1174	1118	-4732.1	2383.8	-1.050	0.371	-0.405	-1.6312	0.8217
HSP90_T2	2589	792	66.8	5110.3	3.267	**0.047***	1.026	0.0265	2.0263

Table 21 *Linear regression analysis of overall tremor (UPDRS) variation and HSP90 expression during pre-operative, early and late post-operative period. Pre-operative and late post-operative HSP90 levels contribute to overall cumulative tremor worsening.*

4.2 Bioinformatics and ML algorithm for prognosticating patient's outcome

From registries query 133 patients resulted with admission diagnosis referable to TBI. According to the abovementioned inclusion and exclusion criteria, from the whole population only 48 patients (33 males, 15 females, mean age 46,5yr) admitted to ER of ARNAS Civico for moderate-severe TBI were included and their data were analyzed. Mean serum albumin on admission was 3,83 g/dL (min 2,4 – max 4,6) and 13 patients experienced hypoalbuminemia during hospitalization. ML algorithm was executed under PyCharm both for mRS and for GOS as final target to be predicted.

The dataset included a total of 48 patients with an initial set of 121 variables (clinical variables such as serum albumin on admission, Glasgow Outcome Scale on admission, mRS and GOS on discharge, radiomic data from brain CT scan and demographics such as sex and age). After data clean up and encoding, the total number of features was extended to 126, including derived or converted columns and spatial coordinates extracted from volumetric segmentation. The target column chosen for classification was the clinical outcome at discharge, firstly measured by modified Rankin Scale (mRS) and then by GOS. There represent ordinal variables reflecting post-traumatic or post-operative functional prognosis.

During preprocessing phase, identifying variables were eliminated, missing values were excluded and numeric variables were normalized in order to make data comparable in terms of scale and distribution. Then, categorical variables were encoded. At the end of this phase, the dataset consisted of 124 features ready for statistical and computational analysis.

Thereafter, dataset dimensionality was reduced and principal features with the greatest impact on variance were identified by *Principal Component Analysis (PCA*). The two main components (PC1 and PC2) resulted from radiomic variables associated with the structure and volumetric texture of the image. These features resulted more sensitive to the internal homogeneity of the lesions.

Once the dataset was reduced by PCA, the data was split into training set and test set in a 70:30 ratio (33 cases for training set and 15 cases for test set). A Random Forest Classifier was trained in order to predict mRS value and GOS value as a multiclass variables, considering each of their values separately.

As regards **mRS** value as target for prognosis estimation, the ML performance analysis highlighted an overall accuracy of 27%, with a highly unbalanced distribution of predictions. In particular, the model showed discriminative ability only on mRS classes 0 and 1, with a recall value of 50% for both, but completely unable to correctly classify classes 2 to 6, for which the recall, precision, and f1-score were equal to 0. The overall macro average f1-score was equal to 0.12, while the weighted average reached a maximum of 0.22. This behavior reflects a substantial inability of the model to generalize the less represented mRS classes because of the small sample size and unbalanced distribution of the target.

The density analysis of the distributions for each feature and for each class made with *seaborn.kdeplot* functions also highlighted that numerous variables had zero or near-zero variance for some classes, which is indicative of poor representativeness in the subsets, further aggravated by the small size of the test set.

Among clinical variables, serum albumin at admission was included as feature and compared with mRS as clinical outcome in multivariate analysis, however albumin did not emerge among the most important features in PCA. **[Table 22]**

Feature	***PC1 Weight***	***PC2 Weight***
glrlm_LongRunHighGrayLevelEmphasis	0.153706	0.017573
glszm_GrayLevelVariance	0.150539	0.061253
glrlm_GrayLevelVariance	0.145241	0.029228
gldm_LargeDependenceHighGrayLevelEmphasis	0.144768	0.144768
glcm_DifferenceVariance	0.144645	0.069167
glszm_SizeZoneNonUniformity	0.137782	0.042709
glcm_Contrast	0.134749	0.085248
glszm_SmallAreaHighGrayLevelEmphasis	0.134540	0.096876
firstorder_Energy	0.133666	0.003386
glcm_ClusterShade	0.133646	0.040345

Table 22. *Top 10 Features of TBI dataset contributing to PCA Components using mRS as target feature for outcome prediction*

Random Forest Classifier showed that several radiomics features are mildly predictive of patient's outcome, considering mRS as target features; in particular shape_MinorAxisLenght showed the greatest importance in predicting patient's outcome. **[Figure 7]** However, overall accuracy of this ML model with mRS as target features showed poor accuracy (0.27) in predicting patient outcome **[Table 23]**

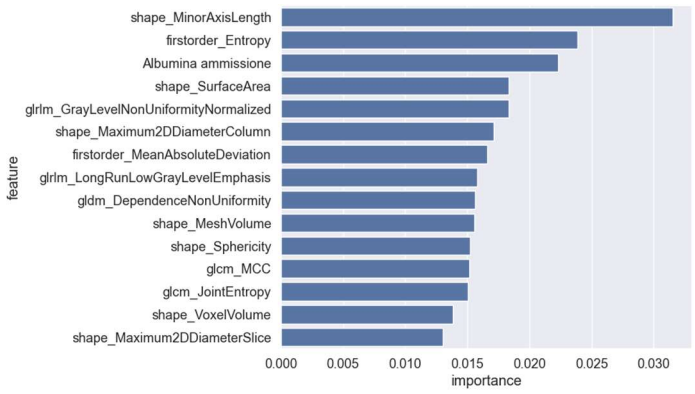

Figure 7 *List of assessment features with greatest importance in predicting patient's outcome considering mRS as target feature*

Class	*Precision*	*Recall*	*F1-score*	*Support (n)*
0	0.40	0.50	0.44	4
1	0.29	0.50	0.36	4
2	0.00	0.00	0.00	2
3	0.00	0.00	0.00	1
4	0.00	0.00	0.00	1
5	0.00	0.00	0.00	1
6	0.00	0.00	0.00	2
Accuracy			0.27	(Total: 15)
Macro Avg	0.10	0.14	0.12	15
Weighted Avg	0.18	0.27	0.22	15

Table 23. *Classification Report assessing predictive accuracy of ML model using mRS as target feature.*

As regards **GOS** as target variable representative of clinical outcome, during the preprocessing GOS was defined as categorical variable wit classes spanning from 1 to 5. Again, distribution among different classes was not homogeneous with low representativity of GOS=2 and GOS=4 and no representativity of GOS=3.

PCA results with GOS as target were comparable to those with mRS, with higher informativity and impact on variance of some radiomics features with slight variations; again, albumin did not result as a major contributor to variance in PCA. **[Table 24]**

Feature	***PC1 Weight***	***PC2 Weight***
glrlm_LongRunHighGrayLevelEmphasis	0.153706	0.017573
glszm_GrayLevelVariance	0.150539	0.061253
glrlm_GrayLevelVariance	0.145241	0.029228
gldm_LargeDependenceHighGrayLevelEmphasis	0.144768	0.060527
glcm_DifferenceVariance	0.144645	0.069167
glszm_SizeZoneNonUniformity	0.137782	0.042709
glszm_SmallAreaHighGrayLevelEmphasis	0.134540	0.096876
firstorder_Energy	0.133666	0.003386
glcm_Contrast	0.134749	0.085248
glcm_ClusterShade	0.133646	0.040345

Table 24. *Top 10 Features of TBI dataset contributing to PCA Components using GOS as target feature for outcome prediction*

After PCA, the reduced dataset was split again into training set and test set in a 70:30 ratio. However, due to the small dataset, test set presented an asymmetric distribution among different classes: GOS=2 (n=2), GOS=4 (n=3), GOS=5 (n=10), and GOS=3 (n=0).

Even in this case, random Forest Classifier showed that several radiomic features are mildly predictive of patient's outcome, considering GOS as target features; in particular shape_Maximun2DDiameter showed the greatest importance in predicting patient's outcome followed by firstorder_Entropy and shape_MinorAxisLenght. **[Figure 8]**

The classification was significantly better using GOS as target than mRS. The overall accuracy of the model reached 67%, indicating greater predictive value compared to the classification on mRS, despite predominantly influenced by GOS=5 class in the test set.

The precision, recall, and f1-score for the GOS=5 class (n=10) were 0.71, 1.00, and 0.83, respectively, indicating the model's ability to correctly recognize favorable outcomes at discharge. As regards worse outcomes, the model was not able to correctly identified GOS=2 and GOS=4 classes which showed an f1-score of 0.

Aggregate metrics for GOS as target showed a macro average f1-score of 0.21 and a weighted average f1-score of 0.56, with a clear improvement over the mRS analysis **[Table 25,26]**.

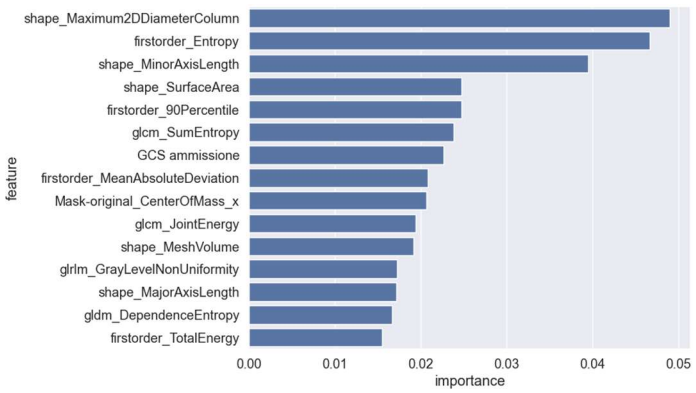

Figure 8 *List of assessment features with greatest importance in predicting patient's outcome considering GOS as target feature*

Class	***Precision***	***Recall***	***F1-score***	***Support (n)***
2	0.00	0.00	0.00	2
3	0.00	0.00	0.00	0
4	0.00	0.00	0.00	3
5	0.71	1.00	0.83	10
Accuracy			0.67	(Total: 15)
Macro Avg	0.18	0.25	0.21	15
Weighted Avg	0.48	0.67	0.56	15

Table 25. *Classification Report assessing predictive accuracy of ML model using GOS as target feature*

Metric	**mRS Target**	**GOS Target**
ACCURACY	0.27	**0.67**
MACRO AVERAGE PRECISION	0.10	0.18
MACRO AVERAGE RECALL	0.14	0.25
MACRO AVERAGE F1-SCORE	0.12	0.21
WEIGHTED AVERAGE PRECISION	0.18	0.48
WEIGHTED AVERAGE RECALL	0.27	0.67
WEIGHTED AVERAGE F1-SCORE	0.22	0.56
BEST PERFORMING CLASS (RECALL)	Class 0 → 0.50	Class 5 → 1.00
UNPREDICTED CLASSES	2, 3, 4, 5, 6	2, 3, 4

Table 26*: Comparison of classification performance according to different target feature. Predictive accuracy of ML model with GOS as target feature outperforms the predictive accuracy considering mRS as target feature.*

5 Discussion

Heat shock proteins (HSPs) represent family of highly conserved proteins, which act as molecular chaperones ensuring protein homeostasis in case of cellular stress. In physiological conditions, HSPs promote the correct folding of new synthetized proteins or refolding of denatured ones, even preventing protein aggregation in neurondegenerative diseases. [158,159] HSPs systemic expression is physiologically promoted by Heat Shock Factor 1 (HSF1), which promotes gene transcription after stressful conditions such as trauma, heat, inflammation and tissue lesions (cytoprotective heat shock response – HSR) in order to protect cell from apoptosis, oxidative stress and acting as immunomodulators. [160,161] In particular, it has been shown that HSP90 plays a critical role in proteostasis by inhibiting HSF1 in unstressed cells, and by stabilizing protein complexes and regulating cellular apoptosis in case of cellular stress. [160,162]

As regard inflammatory response in the central nervous system, it has been shown that HSP90 is overexpressed in case of brain ischemia or injury: in particular, HSP90 seems to be involved in neuroinflammation and response to brain tissue damage through the regulation of several toll-like receptors and NF-kB and promoting microglia activation. [160,163] In models of neurodegenerative diseases, such as PD, HSP90 expression has been linked to α-synuclein metabolism and LRRK and HSP90 inhibition has been linked to neuroprotective effects. [145,164]

From results of this study, early post-operative increase of HSP90 expression is consistent with the already known heat shock response (HSR) after brain lesions or thermal and mechanical stimulation.[165,166] In facts, by the application focal ultrasound, tcMRgFUS thalamotomy may induce a strong cellular stress following localized heating of brain tissue and coagulative necrosis. In facts, it has been shown that the transcranial application of low-intensity pulsed ultrasound may upregulate HSP90 and HSP70 expression in brain tissue secondary to local mechanical or thermal stress along with systemic HSPs regulation secondary to inflammatory response [160,161]. Since these evidences and the upregulation of HSP90 following inflammatory response, in case of tcMRgFUS thalamotomy thermal lesion and oxidative stress may promote HSPs synthesis; in particular, following focused ultrasound thalamotomy, HSPs may be release from the brain tissue surrounding the central core of coagulative necrosis, not from the core itself since high reached temperature (>55°C) which causes protein denaturation.

Among the studied HSPs (HSP27, HSP40 and HSP90), in this study only HSP90 showed significant increase of serum expression after tcMRgFUS thalamotomy in the whole population, more in ET than in PD patients and mostly at 48h from surgery. This evidence suggests that HSP90 participates to an acute response to oxidative and inflammatory surgical stress. Moreover, since only HSP90 showed a significant increase after tcMRgFUS thalamotomy suggest that HSP90 has a lower thermal threshold of activation and its higher expression may prevent other HSPs expression by binding and inactivating HSF1 and inhibiting the cytoprotective HSR. [160,167] According to this hypothesis, higher expression of HSP90 justifies the lack of

HSP40 variation. Unquantifiable expression of HSP27 is consistent to its very low plasmatic level and its predominant intracytoplasmic and intranuclear expression. [139,166]

In our study, HSP90 showed a significant and persistent variation between pre-operative and post-operative time in ET patients and only within the early post-operative time in PD patients. According to the concept of acute cytoprotective heat shock response (HSR), this may suggest that HSP90 may represent an early post-operative marker of surgical stress after tcMRgFUS thalamotomy. However, the significant and persistent post-operative increase of HSP90 in ET patients which corresponds only to an early post-operative increase in PD patients may reflect a different pathophysiology between ET and PD, such as different proteostatic regulation or different molecular environment.

An interesting result from this study is the correlation between post-operative HSP90 expression and clinical outcome with late worsening of tremor. In facts, this study showed that a significant post-operative increase of HSP90 expression is associated with long-term clinical deterioration, such as tremor recurrence or worsening despite an initial clinical improvement after surgery. This relationship suggests that post-operative HSP90 may represent an early negative prognostic marker both in ET and PD patients undergone tcMRgFUS thalamotomy for tremor. This finding is in line with the evidence that higher expression of several HSPs may predict unfavorable outcome in other clinical scenarios such as severe trauma. [161]

However, post-operative HSP90 showed a sort of ceiling effect in prognosticating late clinical outcome when compared to pre-operative levels; in facts, higher pre-operative expression of HSP90 has been related to lower post-operative increase and milder late worsening of tremor. This finding highlights the need to assess cumulative changes of HSP90 expression instead of absolute values and confirms the need of dynamic biomarkers in the prognostication of tremor recurrence after tcMRgFUS thalamotomy for the treatment of both ET and PD tremor.

This negative prognostic capability may be explained by the involvement of HSP90 in neurodegenerative diseases (such as upregulation and accumulation in PD) and the inhibitory effect on HSF1 thus preventing further expression of co-chaperones (such as HSP27 and HSP70) which leads to reduced cellular protection from oxidative stress and sustains cytotoxicity. [144,162] Thus, higher expression of HSP90 may result in maladaptive cellular response in the early post-operative period, maintaining a favorable environment for neuroinflammation and tremor recurrence.

Interestingly, it has been shown that HSP90 is involved both in physiologic synaptic regulation and synaptic rearrangement after brain injury; in particular, the inhibition of HSP90 seems to promote synaptic rearrangement and formation of dendritic spikes through an HSF-1 dependent pathway in experimental model of neurodegenerative disease. [168–170] Thus, the post-operative over-expression of HSP90 may be related to late clinical worsening and tremor recurrence because of sustained and amplified neuroinflammatory response; in this inflammatory environment, synaptic rearrangement may promote an escaping mechanism which may bypass the former brain lesion and its interrupted pathways; thus, tremor recurrence may be promoted by

aberrant brain connectivity rather than small lesion volume, inappropriate targeting or disease progression, which potentially sustains former pathological network and invalidates early post-operative tremor improvement.[117,120,121]

In the available literature about tcMRgFUS for the treatment of tremor, technical parameters (e.g. lesion volume, focal temperature, target localization), advanced neuroimaging or patient's characteristics (e.g. age, tremor rate) have been mostly investigated as possible predictors of clinical outcomes. [120] However, no molecular marker has been yet investigated nor artificial intelligence algorithm has been developed in order to assess possible prognostic features, despite the high rate (up to 5%) of long-term tremor recurrence and further evidences of HSPs negative prognostic capability in other clinical scenarios. [120,161]

Therefore, the results of this study offer a new insight on the role of HSP90 as potential molecular biomarker of cellular stress response with negative prognostic value in patients undergoing tcMRgFUS thalamotomy for tremor. This evidence enriches the knowledge about molecular response to this surgical technique, shedding light on the role of cellular stress and long-term clinical outcome in neurodegenerative diseases. However, this evidence represents only a path: further research and studies will be needed in order to validate these findings in larger population, including other markers of cellular stress and neuroinflammation to completely depict the profile of molecular pathophysiology of movement disorders and the systemic response to tcMRgFUS thalamotomy.

In parallel, within the aims of this study, an ML algorithm was developed in order to enhance prognostic capability in patients undergone tcMRgFUS thalamotomy for tremor and to further investigate serum markers and radiomics data as potential early prognostic features for clinical outcome. Since the very limited population of ET and PD patients, this ML algorithm was developed and tested on a "mock" dataset consisting of TBI patients in order to demonstrate the reproducibility and general applicability of the same approach. In this scenario, albumin was used as serum markers in place of HSP, GOS and mRS were used as outcome indicators in place of clinical score for tremor; as regard neuroimaging, radiomics data were analyzed from post-TBI brain CT in place of post-operative brain MRI of ET and PD patients.

This pipeline developed on TBI dataset demonstrated that outcome variance was mainly influenced by texture-based features extracted from PyRadiomics. However, the classification on a small sample of 48 patients showed limited generalizability. Thus, performance of this ML algorithm may be improved with larger dataset.

AI algorithm based on radiomics and ML ensures the extraction of quantitative data which may be missed by clinical eye and the building of robust predictive model from their integration with clinical and molecular data. The predictive and diagnostic capabilities of radiomics in neurosciences have been already reported, however the risk of overfitting is high in case of large number of features exceeding the number of cases. Thus, robustness, reproducibility and generalizability of ML algorithm based on radiomics relies on large and standardized datasets according to IBSI guidelines, and on multicenter external validation. [148,152,171–177]

In this study, TBI was adopted as mock scenario since the proof-of-concept design and the wider dataset available for training in order to validate the whole analytical pipeline (from brain segmentation, to radiomics extraction, preprocessing of radiomic data, analysis of principal components and classification). However, even with this strategy, 48 cases of TBI dataset were not sufficient to complete ML stratification through Random Forest classifier obtaining a stratification for outcome target features. Moreover, the accuracy was higher considering GOS as target feature for outcome prognostication (which is a general outcome score) because of low variability of dataset which prevents proper stratification and classification according to mRS (which is more representative of neurological outcome), thus larger dataset is needed in order to ensure variability and generalizability even for neurological outcome. In addition to dataset dimensionality, considering the rampant developing of ML algorithm and the wider use of AI in several fields of medical and biological sciences, it seems to be mandatory to adopt standardized pipelines, quality control of selected features and cross validation techniques on independent cohort, in order to obtain robust, reliable and generalizable algorithm in the era of precision and personalized medicine.

Moreover, the availability of an early marker which can stratify the risk of tremor recurrence would significantly impact clinical course of patients undergone tcMRgFUS with precise candidate selection for further treatment, customization of energy dose or target, closer follow-up or additional therapies such as retreatment, retargeting or secondary DBS. A measurable molecular marker from peripheral blood flow such as HSP90, combined with radiomics and analysis of pre-operative patient's characteristics (with advanced neuroimaging and individual clinical data) and procedural parameters (such as targeting, energy, temperature and number of sonications) in the same ML algorithm may offer a robust non-invasive and reproducible prognostic and decision-making tool. In this rich and complicate scenario made of several and multimodal features, AI would be responsible for recognizing complex and non-linear patterns which may escape conventional statistical analysis, however large dataset, reproducible pipelines, independent cohorts for adequate training and multicenter validation are needed for the transition to clinical practice.

This study as proof of concept suffers from several limitations. First, as intrinsic limitation, HSP90 is systemically expressed and the specificity for brain tissue is somehow limited by peripheral blood sampling. However, the evidence of peripheral expression of HSP90 and its variations after tcMRgFUS thalamotomy may pave the way for further and more specific evaluations (e.g. brain exosomal HSPs and miRNA). Moreover, serum expression of HSP90 may be adopted as valuable test for the early evaluation of clinical response in order to address closer follow up, possible early re-treatment or pharmacological modulation of HSP90 in order to improve molecular response to tcMRgFUS thalamotomy and patient's clinical outcome since early post-operative period.

Then, the small population made only of 7 ET and 7 PD patients may affect the cause-effect link and limit the interpretation of results since possible confounding variables (targeting, lesion dimension, procedural parameters, systemic comorbidities) and risk of selection bias which are not mitigated by the limited number of samples and the lack of external validation.

Lastly, among evaluated HSPs, the very low sensitivity threshold prevented HSP27 to be evaluated for the entire population, thus limiting by one third the diagnostic potential of this study.

As regard the ML algorithm for prognosticating patient's outcome after TBI, despite the complete and robust pipeline, it showed several limitations such as low variability of training set, not significant or no variance in some classes and disproportion among different classes in the test set.

Considered together, most of these limitations may be further addressed and mitigated by larger and multicentric cohort of tcMRgFUS patients and TBI patients, standardized protocol for radiomic analysis in order to ensure inter-center comparability according to IBSI standards, multimodal integration of advanced neuroimaging and biomolecular markers with procedural parameters, clinical features and advanced imaging, and final external validation of the integrated algorithm.

6 Conclusions

This study evidences the role of HSPs in the pathophysiology of ET and PD tremor of patients undergone tcMRgFUS thalamotomy. The results suggest that HSP90 serum expression responds to the focused ultrasound thalamotomy and its post-operative increase is a predictor of long-term clinical outcome. These findings shed lights to the wide environment of neuronal stress: on one hand, they confirm that HSP90 is a crucial regulator of proteostasis even in movement disorders; on the other, they suggest that HSP90 may represent an early negative prognostic marker since its circulating levels of HSP90 may reflect the severity of post-surgical neuronal stress and predict the risk of tremor recurrence. However, these findings need further investigations with larger cohorts, multimodal features and cross validation in order to be later adopt in clinical practice.

The integration of AI in the evaluation of patient prognosis after tcMRgFUS thalamotomy represent ad advancement in personalized medicine and neurosciences, since the capability of supervised ML algorithm can extract complex patterns and detect subtle correlations from clinical and radiological data which are often non immediately recognizable. However, it must be emphasized that implementation of ML algorithm in clinical practice requires large dataset, rigorous data management, reproducible pipelines and cross validation in order to ensure clinical reliability.

In conclusion, the integrated evaluation of an early circulating molecular marker and the radiomics analysis combined in a robust ML pipelines may offer a powerful and reliable prognostic tool, capable of improving diagnostic accuracy, supporting clinical decisions and optimizing patient's clinical outcomes in a personalized medicine way more precise than before.

7 References

1. Okelberry, T.; Lyons, K.E.; Pahwa, R. Updates in Essential Tremor. *Parkinsonism Relat Disord* 2024, *122*.

2. Shanker, V. Essential Tremor: Diagnosis and Management. *The BMJ* **2019**, *366*, doi:10.1136/bmj.l4485.

3. Louis, E.D.; McCreary, M. How Common Is Essential Tremor? Update on the Worldwide of Essential Tremor. *Tremor Other Hyperkinet. Mov. (N. Y.)* **2021**, *11*, 28.

4. Welton, T.; Cardoso, F.; Carr, J.A.; Chan, L.L.; Deuschl, G.; Jankovic, J.; Tan, E.K. Essential Tremor. *Nat Rev Dis Primers* **2021**, *7*, doi:10.1038/s41572-021-00314-w.

5. Louis, E.D.; Barnes, L.; Albert, S.M.; Cote, L.; Schneier, F.R.; Pulman, S.L.; Yu, Q. Correlates of Functional Disability in Essential Tremor. *Movement Disorders* **2001**, *16*, doi:10.1002/mds.1184.

6. Bain, P.G.; Findley, L.J.; Thompson, P.D.; Gresty, M.A.; Rothwell, J.C.; Harding, A.E.; Marsden, C.D. A Study of Hereditary Essential Tremor. *Brain* **1994**, *117*, doi:10.1093/brain/117.4.805.

7. Koller, W.C.; Busenbark, K.; Miner, K. The Relationship of Essential Tremor to Other Movement Disorders: Report on 678 Patients. *Ann Neurol* **1994**, *35*, doi:10.1002/ana.410350613.

8. Rajput, A.; Robinson, C.A.; Rajput, A.H. Essential Tremor Course and Disability: A Clinicopathologic Study of 20 Cases. *Neurology* **2004**, *62*, doi:10.1212/01.WNL.0000115145.18830.1A.

9. Louis, E.D.; Dogu, O. Does Age of Onset in Essential Tremor Have a Bimodal Distribution? Data from a Tertiary Referral Setting and a Population-Based Study. *Neuroepidemiology* **2008**, *29*, 208–212, doi:10.1159/000111584.

10. Pan, M.K.; Kuo, S.H. Essential Tremor: Clinical Perspectives and Pathophysiology. *J Neurol Sci* 2022, *435*.

11. Kuo, S.H.; Wang, J.; Tate, W.J.; Pan, M.K.; Kelly, G.C.; Gutierrez, J.; Cortes, E.P.; Vonsattel, J.P.G.; Louis, E.D.; Faust, P.L. Cerebellar Pathology in Early Onset and Late Onset Essential Tremor. *Cerebellum* **2017**, *16*, doi:10.1007/s12311-016-0826-5.

12. Louis, E.D.; Vonsattel, J.P.G. The Emerging Neuropathology of Essential Tremor. *Movement Disorders* 2008, *23*.

13. Shill, H.A.; Adler, C.H.; Sabbagh, M.N.; Connor, D.J.; Caviness, J.N.; Hentz, J.G.; Beach, T.G. Pathologic Findings in Prospectively Ascertained Essential Tremor Subjects. *Neurology* **2008**, *70*, doi:10.1212/01.wnl.0000310425.76205.02.

14. Babij, R.; Lee, M.; Cortés, E.; Vonsattel, J.P.G.; Faust, P.L.; Louis, E.D. Purkinje Cell Axonal Anatomy: Quantifying Morphometric Changes in Essential Tremor versus Control Brains. *Brain* **2013**, *136*, doi:10.1093/brain/awt238.

15. Yu, M.; Ma, K.; Faust, P.L.; Honig, L.S.; Cortés, E.; Vonsattel, J.P.G.; Louis, E.D. Increased Number of Purkinje Cell Dendritic Swellings in Essential Tremor. *Eur J Neurol* **2012**, *19*, doi:10.1111/j.1468-1331.2011.03598.x.

16. Lang-Ouellette, D.; Gruver, K.M.; Smith-Dijak, A.; Blot, F.G.C.; Stewart, C.A.; de Vanssay de Blavous, P.; Li, C.H.; Van Eitrem, C.; Rosen, C.; Faust, P.L.; et al. Purkinje Cell Axonal Swellings Enhance Action Potential Fidelity and Cerebellar Function. *Nat Commun* **2021**, *12*, doi:10.1038/s41467-021-24390-4.

17. Louis, E.D.; Zheng, W.; Mao, X.; Shungu, D.C. Blood Harmane Is Correlated with Cerebellar Metabolism in Essential Tremor: A Pilot Study. *Neurology* **2007**, *69*, doi:10.1212/01.wnl.0000266663.27398.9f.

18. Pan, M.K.; Li, Y.S.; Wong, S.B.; Ni, C.L.; Wang, Y.M.; Liu, W.C.; Lu, L.Y.; Lee, J.C.; Cortes, E.P.; Vonsattel, J.P.G.; et al. Cerebellar Oscillations Driven by Synaptic Pruning Deficits of Cerebellar Climbing Fibers Contribute to Tremor Pathophysiology. *Sci Transl Med* **2020**, *12*, doi:10.1126/scitranslmed.aay1769.

19. Ma, S.; Davis, T.L.; Blair, M.A.; Fang, J.Y.; Bradford, Y.; Haines, J.L.; Hedera, P. Familial Essential Tremor with Apparent Autosomal Dominant Inheritance: Should We Also Consider Other Inheritance Modes? *Movement Disorders* **2006**, *21*, doi:10.1002/mds.20950.

20. Deng, H.; Le, W.; Jankovic, J. Genetics of Essential Tremor. *Brain* **2007**, *130*, 1456–1464.

21. Higgins, J.J.; Pho, L.T.; Nee, L.E. A Gene (ETM) for Essential Tremor Maps to Chromosome 2p22-P25. *Movement Disorders* 1997, *12*.

22. Shatunov, A.; Sambuughin, N.; Jankovic, J.; Elble, R.; Lee, H.S.; Singleton, A.B.; Dagvadorj, A.; Ji, J.; Zhang, Y.; Kimonis, V.E.; et al. Genomewide Scans in North American Families Reveal Genetic Linkage of Essential Tremor to a Region on Chromosome 6p23. *Brain* **2006**, *129*, doi:10.1093/brain/awl120.

23. Parmalee, N.; Mirzozoda, K.; Kisselev, S.; Merner, N.; Dion, P.; Rouleau, G.; Clark, L.; Louis, E.D. Genetic Analysis of the FUS/TLS Gene in Essential Tremor. *Eur J Neurol* **2013**, *20*, doi:10.1111/ene.12023.

24. Deng, H.; Gu, S.; Jankovic, J. LINGO1 Variants in Essential Tremor and Parkinson's Disease. *Acta Neurol Scand* 2012, *125*.

25. Delay, C.; Tremblay, C.; Brochu, E.; Paris-Robidas, S.; Emond, V.; Rajput, A.H.; Rajput, A.; Calon, F. Increased LINGO1 in the Cerebellum of Essential Tremor Patients. *Movement Disorders* **2014**, *29*, doi:10.1002/mds.25819.

26. Chi, W.; Wu, M.; Wang, H. lu; Wu, Q. yan; Zhang, Y. ping; Hu, Y. nan; Zhu, Y. bin; Lin, X. fu; Chen, T.; Luo, J. wei; et al. Han Family with Essential Tremor Caused by the P421L Variant of the TENM4 Gene in China. *Neurological Sciences* **2023**, *44*, doi:10.1007/s10072-023-06603-4.

27. Koller, W.C.; Vetere-Overfield, B. Acute and Chronic Effects of Propranolol and Primidone in Essential Tremor. *Neurology* **1989**, *39*, doi:10.1212/wnl.39.12.1587.

28. Winkler, G.F.; Young, R.R. Efficacy of Chronic Propranolol Therapy in Action Tremors of the Familial, Senile or Essential Varieties. *New England Journal of Medicine* **1974**, *290*, doi:10.1056/nejm197405022901802.

29. Teräväinen, H.; Fogelholm, R.; Larsen, A. Effect of Propranolol on Essential Tremor. *Neurology* **1976**, *26*, doi:10.1212/wnl.26.1.27.

30. Ondo, W.; Jankovic, J.; Schwartz, K.; Almaguer, M.; Simpson, R.K. Unilateral Thalamic Deep Brain Stimulation for Refractory Essential Tremor and Parkinson's Disease Tremor. *Neurology* **1998**, *51*, doi:10.1212/WNL.51.4.1063.

31. Fytagoridis, A.; Sandvik, U.; Åström, M.; Bergenheim, T.; Blomstedt, P. Long Term Follow-up of Deep Brain Stimulation of the Caudal Zona Incerta for Essential Tremor. *J Neurol Neurosurg Psychiatry* **2012**, *83*, doi:10.1136/jnnp-2011-300765.

32. Shashkin, C. Complications of Deep Brain Stimulation for Movement Disorders: Literature Review and Personal Experience. In *Acta Neurochirurgica, Supplementum*; 2023; Vol. 130.

33. Rasiah, N.P.; Maheshwary, R.; Kwon, C.S.; Bloomstein, J.D.; Girgis, F. Complications of Deep Brain Stimulation for Parkinson Disease and Relationship between Micro-Electrode Tracks and Hemorrhage: Systematic Review and Meta-Analysis. *World Neurosurg* **2023**, *171*, doi:10.1016/j.wneu.2022.10.034.

34. Barbe, M.T.; Liebhart, L.; Runge, M.; Pauls, K.A.M.; Wojtecki, L.; Schnitzler, A.; Allert, N.; Fink, G.R.; Sturm, V.; Maarouf, M.; et al. Deep Brain Stimulation in the Nucleus Ventralis Intermedius in Patients with Essential Tremor: Habituation of Tremor Suppression. *J Neurol* **2011**, *258*, doi:10.1007/s00415-010-5773-3.

35. Fasano, A.; Helmich, R.C. Tremor Habituation to Deep Brain Stimulation: Underlying Mechanisms and Solutions. *Movement Disorders* **2019**, *34*, 1761–1773, doi:10.1002/mds.27821.

36. Peters, J.; Tisch, S. Habituation After Deep Brain Stimulation in Tremor Syndromes: Prevalence, Risk Factors and Long-Term Outcomes. *Front Neurol* 2021, *12*.

37. Grewal, S.S.; Domingo, R.A.; Wharen, R.E. Left Radiofrequency Thalamotomy for Drug-Refractory Essential Tremor. *World Neurosurg* **2020**, *134*, doi:10.1016/j.wneu.2019.10.180.

38. Wirth, T.; Goedemans, T.; Rajabian, A.; Dayal, V.; Abuhusain, H.; Vijiaratnam, N.; Athauda, D.; Hariz, M.; Foltynie, T.; Limousin, P.; et al. Clinical Outcomes after MRI Connectivity-Guided Radiofrequency Thalamotomy for Tremor. *J Neurosurg* **2024**, *140*, doi:10.3171/2023.7.JNS222744.

39. Shaikh, A.A.; Querejetacoma, A.; Petric, B.; Sarangmat, N.; Aziz, T.Z.; Fitzgerald, J.J.; Bogdanovic, M.; Pereira, E.A.; Green, A.L. Radiofrequency Thalamotomy for Tremor Outcomes Correlate with dentorubrothalamic Tract Distance. *Br. J. Neurosurg.* **2025**, 1–10.

40. Onder, H.; Kocer, B.; Comoglu, S. Early Recurrence of Holmes Tremor after Radiofrequency Thalamotomy. *Ann Indian Acad Neurol* **2022**, *25*, doi:10.4103/aian.aian_1107_21.

41. Pauwels, R.W.J.; Oterdoom, D.L.M.; Drost, G.; Van Laar, T.; Van Dijk, J.M.C. Long-Term Patient-Reported Outcome of Radiofrequency Thalamotomy for Tremor. *Stereotact Funct Neurosurg* **2020**, *98*, doi:10.1159/000506999.

42. Dallapiazza, R.F.; Lee, D.J.; De Vloo, P.; Fomenko, A.; Hamani, C.; Hodaie, M.; Kalia, S.K.; Fasano, A.; Lozano, A.M. Outcomes from Stereotactic Surgery for Essential Tremor. *J Neurol Neurosurg Psychiatry* 2019, *90*, 474–482.

43. Giammalva, G.R.; Maugeri, R.; Umana, G.E.; Paolini, F.; Bonosi, L.; Meccio, F.; Scalia, G.; Palmisciano, P.; Gerardi, R.M.; Iacopino, D.G. DBS, TcMRgFUS, and Gamma Knife Radiosurgery for the Treatment of Essential Tremor: A Systematic Review on Techniques, Indications, and Current Applications. *J Neurosurg Sci* 2022, *66*.

44. Shih, L.C.; LaFaver, K.; Lim, C.; Papavassiliou, E.; Tarsy, D. Loss of Benefit in VIM Thalamic Deep Brain Stimulation (DBS) for Essential Tremor(ET): How Prevalent Is It? *Parkinsonism Relat Disord* **2013**, *19*, doi:10.1016/j.parkreldis.2013.03.006.

45. Blomstedt, P.; Hariz, G.M.; Hariz, M.I.; Koskinen, L.O.D. Thalamic Deep Brain Stimulation in the Treatment of Essential Tremor: A Long-Term Follow-Up. *Br J Neurosurg* **2007**, *21*, 504–509, doi:10.1080/02688690701552278.

46. Pahwa, R.; Lyons, K.E.; Wilkinson, S.B.; Simpson, R.K.; Ondo, W.G.; Tarsy, D.; Norregaard, T.; Hubble, J.P.; Smith, D.A.; Hauser, R.A.; et al. Long-Term Evaluation of Deep Brain Stimulation of the Thalamus. *J Neurosurg* **2006**, *104*, 506–512, doi:10.3171/jns.2006.104.4.506.

47. Nazzaro, J.M.; Pahwa, R.; Lyons, K.E. Long-Term Benefits in Quality of Life after Unilateral Thalamic Deep Brain Stimulation for Essential Tremor: Clinical Article. *J Neurosurg* **2012**, *117*, doi:10.3171/2012.3.JNS112316.

48. Cury, R.G.; Fraix, V.; Castrioto, A.; Pérez Fernández, M.A.; Krack, P.; Chabardes, S.; Seigneuret, E.; Alho, E.J.L.; Benabid, A.L.; Moro, E. Thalamic Deep Brain Stimulation for Tremor in Parkinson Disease, Essential Tremor, and Dystonia. *Neurology* **2017**, *89*, 1416–1423, doi:10.1212/WNL.0000000000004295.

49. Baizabal-Carvallo, J.F.; Kagnoff, M.N.; Jimenez-Shahed, J.; Fekete, R.; Jankovic, J. The Safety and Efficacy of Thalamic Deep Brain Stimulation in Essential Tremor: 10 Years and Beyond. *J Neurol Neurosurg Psychiatry* **2014**, *85*, doi:10.1136/jnnp-2013-304943.

50. Picillo, M.; Lozano, A.M.; Kou, N.; Munhoz, R.P.; Fasano, A. Programming Deep Brain Stimulation for Tremor and Dystonia: The Toronto Western Hospital Algorithms. *Brain Stimul* 2016, *9*.

51. Akbostanci, M.C.; Slavin, K. V.; Burchiel, K.J. Stereotactic Ventral Intermedial Thalamotomy for the Treatment of Essential Tremor: Results of a Series of 37 Patients. In Proceedings of the Stereotactic and Functional Neurosurgery; 1999; Vol. 72.

52. Armstrong, M.J.; Okun, M.S. Diagnosis and Treatment of Parkinson Disease: A Review. *JAMA - Journal of the American Medical Association* 2020, *323*.

53. Bloem, B.R.; Okun, M.S.; Klein, C. Parkinson's Disease. *Lancet* **2021**, *397*, 2284–2303, doi:10.1016/S0140-6736(21)00218-X.

54. Santos García, D.; de Deus Fonticoba, T.; Suárez Castro, E.; Borrué, C.; Mata, M.; Solano Vila, B.; Cots Foraster, A.; Álvarez Sauco, M.; Rodríguez Pérez, A.B.; Vela, L.; et al. Non-Motor Symptoms Burden, Mood, and Gait Problems Are the Most Significant Factors Contributing to a Poor Quality of Life in Non-Demented Parkinson's Disease Patients: Results from the COPPADIS Study Cohort. *Parkinsonism Relat Disord* **2019**, *66*, doi:10.1016/j.parkreldis.2019.07.031.

55. Shahmoradian, S.H.; Lewis, A.J.; Genoud, C.; Hench, J.; Moors, T.E.; Navarro, P.P.; Castaño-Díez, D.; Schweighauser, G.; Graff-Meyer, A.; Goldie, K.N.; et al. Lewy Pathology in Parkinson's Disease Consists of Crowded Organelles and Lipid Membranes. *Nat Neurosci* **2019**, *22*, doi:10.1038/s41593-019-0423-2.

56. Chahine, L.M.; Beach, T.G.; Brumm, M.C.; Adler, C.H.; Coffey, C.S.; Mosovsky, S.; Caspell-Garcia, C.; Serrano, G.E.; Munoz, D.G.; White, C.L.; et al. In Vivo Distribution of α-Synuclein in Multiple Tissues and Biofluids in Parkinson Disease. *Neurology* **2020**, *95*, doi:10.1212/WNL.0000000000010404.

57. Pringsheim, T.; Jette, N.; Frolkis, A.; Steeves, T.D.L. The Prevalence of Parkinson's Disease: A Systematic Review and Meta-Analysis. *Movement Disorders* 2014, *29*.

58. Deuschl, G.; Beghi, E.; Fazekas, F.; Varga, T.; Christoforidi, K.A.; Sipido, E.; Bassetti, C.L.; Vos, T.; Feigin, V.L. The Burden of Neurological Diseases in Europe: An Analysis for the Global Burden of Disease Study 2017. *Lancet Public Health* **2020**, *5*, doi:10.1016/S2468-2667(20)30190-0.

59. Bjornestad, A.; Forsaa, E.B.; Pedersen, K.F.; Tysnes, O.B.; Larsen, J.P.; Alves, G. Risk and Course of Motor Complications in a Population-Based Incident Parkinson's Disease Cohort. *Parkinsonism Relat Disord* **2016**, *22*, doi:10.1016/j.parkreldis.2015.11.007.

60. Picillo, M.; Palladino, R.; Moccia, M.; Erro, R.; Amboni, M.; Vitale, C.; Barone, P.; Pellecchia, M.T. Gender and Non Motor Fluctuations in Parkinson's Disease: A Prospective Study. *Parkinsonism Relat Disord* **2016**, *27*, doi:10.1016/j.parkreldis.2016.04.001.

61. Nicoletti, A.; Vasta, R.; Mostile, G.; Nicoletti, G.; Arabia, G.; Iliceto, G.; Lamberti, P.; Marconi, R.; Morgante, L.; Barone, P.; et al. Gender Effect on Non-Motor Symptoms in Parkinson's Disease: Are Men More at Risk? *Parkinsonism Relat Disord* **2017**, *35*, doi:10.1016/j.parkreldis.2016.12.008.

62. Trinh, J.; Zeldenrust, F.M.J.; Huang, J.; Kasten, M.; Schaake, S.; Petkovic, S.; Madoev, H.; Grünewald, A.; Almuammar, S.; König, I.R.; et al. Genotype-Phenotype Relations for the Parkinson's Disease Genes SNCA, LRRK2, VPS35: MDSGene Systematic Review. *Movement Disorders* 2018, *33*.

63. Kasten, M.; Hartmann, C.; Hampf, J.; Schaake, S.; Westenberger, A.; Vollstedt, E.J.; Balck, A.; Domingo, A.; Vulinovic, F.; Dulovic, M.; et al. Genotype-Phenotype Relations for the Parkinson's Disease Genes Parkin, PINK1, DJ1: MDSGene Systematic Review. *Movement Disorders* 2018, *33*.

64. Skrahina, V.; Gaber, H.; Vollstedt, E.J.; Förster, T.M.; Usnich, T.; Curado, F.; Brüggemann, N.; Paul, J.; Bogdanovic, X.; Zülbahar, S.; et al. The Rostock International Parkinson's Disease (ROPAD) Study: Protocol and Initial Findings. *Movement Disorders* **2021**, *36*, doi:10.1002/mds.28416.

65. Ryan, E.; Seehra, G.; Sharma, P.; Sidransky, E. GBA1 -Associated Parkinsonism: New Insights and Therapeutic Opportunities. *Curr Opin Neurol* 2019, *32*.

66. Nonnekes, J.; Post, B.; Tetrud, J.W.; Langston, J.W.; Bloem, B.R. MPTP-Induced Parkinsonism: An Historical Case Series. *Lancet Neurol* 2018, *17*.

67. Cohen, M.E.; Eichel, R.; Steiner-Birmanns, B.; Janah, A.; Ioshpa, M.; Bar-Shalom, R.; Paul, J.J.; Gaber, H.; Skrahina, V.; Bornstein, N.M.; et al. A Case of Probable Parkinson's Disease after SARS-CoV-2 Infection. *Lancet Neurol* 2020, *19*.

68. Merello, M.; Bhatia, K.P.; Obeso, J.A. SARS-CoV-2 and the Risk of Parkinson's Disease: Facts and Fantasy. *Lancet Neurol* **2021**, *20*, doi:10.1016/S1474-4422(20)30442-7.

69. Brundin, P.; Nath, A.; Beckham, J.D. Is COVID-19 a Perfect Storm for Parkinson's Disease? *Trends Neurosci* 2020, *43*.

70. Noyce, A.J.; Bestwick, J.P.; Silveira-Moriyama, L.; Hawkes, C.H.; Giovannoni, G.; Lees, A.J.; Schrag, A. Meta-Analysis of Early Nonmotor Features and Risk Factors for Parkinson Disease. *Ann Neurol* 2012, *72*.

71. Kalia, L. V.; Lang, A.E. Parkinson's Disease. *The Lancet* 2015, *386*.

72. Dirkx, M.F.; Bologna, M. The Pathophysiology of Parkinson's Disease Tremor. *J Neurol Sci* 2022, *435*.

73. Gigante, A.F.; Pellicciari, R.; Iliceto, G.; Liuzzi, D.; Mancino, P.V.; Custodero, G.E.; Guido, M.; Livrea, P.; Defazio, G. Rest Tremor in Parkinson's Disease: Body Distribution and Time of Appearance. *J Neurol Sci* **2017**, *375*, doi:10.1016/j.jns.2016.12.057.

74. Zach, H.; Dirkx, M.F.; Pasman, J.W.; Bloem, B.R.; Helmich, R.C. Cognitive Stress Reduces the Effect of Levodopa on Parkinson's Resting Tremor. *CNS Neurosci Ther* **2017**, *23*, doi:10.1111/cns.12670.

75. Selikhova, M.; Williams, D.R.; Kempster, P.A.; Holton, J.L.; Revesz, T.; Lees, A.J. A Clinico-Pathological Study of Subtypes in Parkinson's Disease. *Brain* **2009**, *132*, doi:10.1093/brain/awp234.

76. Fishman, P.S. Paradoxical Aspects of Parkinsonian Tremor. *Movement Disorders* 2008, *23*.

77. García-Cabezas, M.Á.; Rico, B.; Sánchez-González, M.Á.; Cavada, C. Distribution of the Dopamine Innervation in the Macaque and Human Thalamus. *Neuroimage* **2007**, *34*, doi:10.1016/j.neuroimage.2006.07.032.

78. Sánchez-González, M.Á.; García-Cabezas, M.Á.; Rico, B.; Cavada, C. The Primate Thalamus Is a Key Target for Brain Dopamine. *Journal of Neuroscience* **2005**, *25*, doi:10.1523/JNEUROSCI.0968-05.2005.

79. Dirkx, M.F.; Den Ouden, H.E.M.; Aarts, E.; Timmer, M.H.M.; Bloem, B.R.; Toni, I.; Helmich, R.C. Dopamine Controls Parkinson's Tremor by Inhibiting the Cerebellar Thalamus. *Brain* **2017**, *140*, doi:10.1093/brain/aww331.

80. Magnin, M.; Morel, A.; Jeanmonod, D. Single-Unit Analysis of the Pallidum, Thalamus and Subthalamic Nucleus in Parkinsonian Patients. *Neuroscience* **2000**, *96*, doi:10.1016/S0306-4522(99)00583-7.

81. Moran, A.; Bergman, H.; Israel, Z.; Bar-Gad, I. Subthalamic Nucleus Functional Organization Revealed by Parkinsonian Neuronal Oscillations and Synchrony. *Brain* **2008**, *131*, doi:10.1093/brain/awn270.

82. Amtage, F.; Henschel, K.; Schelter, B.; Vesper, J.; Timmer, J.; Lücking, C.H.; Hellwig, B. Tremor-Correlated Neuronal Activity in the Subthalamic Nucleus of Parkinsonian Patients. *Neurosci Lett* **2008**, *442*, doi:10.1016/j.neulet.2008.06.087.

83. Asch, N.; Herschman, Y.; Maoz, R.; Auerbach-Asch, C.R.; Valsky, D.; Abu-Snineh, M.; Arkadir, D.; Linetsky, E.; Eitan, R.; Marmor, O.; et al. Independently Together: Subthalamic Theta and Beta

Opposite Roles in Predicting Parkinson's Tremor. *Brain Commun* **2020**, *2*, doi:10.1093/braincomms/fcaa074.

84. Anastasopoulos, D. Tremor in Parkinson's Disease May Arise from Interactions of Central Rhythms with Spinal Reflex Loop Oscillations. *J Parkinsons Dis* 2020, *10*.

85. Volkmann, J.; Joliot, M.; Mogilner, A.; Ioannides, A.A.; Lado, F.; Fazzini, E.; Ribary, U.; Llinás, R. Central Motor Loop Oscillations in Parkinsonian Resting Tremor Revealed by Magnetoencephalography. *Neurology* **1996**, *46*, doi:10.1212/wnl.46.5.1359.

86. Helmich, R.C.; Hallett, M.; Deuschl, G.; Toni, I.; Bloem, B.R. Cerebral Causes and Consequences of Parkinsonian Resting Tremor: A Tale of Two Circuits? *Brain* 2012, *135*.

87. Nemade, D.; Subramanian, T.; Shivkumar, V. An Update on Medical and Surgical Treatments of Parkinson's Disease. *Aging Dis* 2021, *12*.

88. Poewe, W.; Antonini, A.; Zijlmans, J.C.; Burkhard, P.R.; Vingerhoets, F. Levodopa in the Treatment of Parkinson's Disease: An Old Drug Still Going Strong. *Clin Interv Aging* 2010, *5*.

89. Lachenmayer, M.L.; Bettschen, C.; Bernasconi, C.; Petermann, K.; Debove, I.; Muellner, J.; Michelis, J.P.; Burgunder, J.M.; Krauss, J.K.; Oertel, M.F.; et al. Stimulation of the Globus Pallidus Internus in the Treatment of Parkinson's Disease: Long-Term Results of a Monocentric Cohort. *Parkinsonism Relat Disord* **2019**, *64*, doi:10.1016/j.parkreldis.2019.03.009.

90. Limousin, P.; Foltynie, T. Long-Term Outcomes of Deep Brain Stimulation in Parkinson Disease. *Nat Rev Neurol* 2019, *15*.

91. Ramirez-Zamora, A.; Ostrem, J.L. Globus Pallidus Interna or Subthalamic Nucleus Deep Brain Stimulation for Parkinson Disease a Review. *JAMA Neurol* 2018, *75*.

92. Odekerken, V.J.J.; van Laar, T.; Staal, M.J.; Mosch, A.; Hoffmann, C.F.E.; Nijssen, P.C.G.; Beute, G.N.; van Vugt, J.P.P.; Lenders, M.W.P.M.; Contarino, M.F.; et al. Subthalamic Nucleus versus Globus Pallidus Bilateral Deep Brain Stimulation for Advanced Parkinson's Disease (NSTAPS Study): A Randomised Controlled Trial. *Lancet Neurol* **2013**, *12*, doi:10.1016/S1474-4422(12)70264-8.

93. Maamary, J.; Peters, J.; Kyle, K.; Barnett, Y.; Jonker, B.; Tisch, S. Effective Subthalamic Nucleus Deep Brain Stimulation Following MRgFUS for Tremor Dominant Parkinson's Disease. *Mov Disord Clin Pract* **2023**, *10*, doi:10.1002/mdc3.13662.

94. Saluja, S.; Barbosa, D.A.N.; Parker, J.J.; Huang, Y.; Jensen, M.R.; Ngo, V.; Santini, V.E.; Pauly, K.B.; Ghanouni, P.; McNab, J.A.; et al. Case Report on Deep Brain Stimulation Rescue After Suboptimal MR-Guided Focused Ultrasound Thalamotomy for Essential Tremor: A Tractography-Based Investigation. *Front Hum Neurosci* **2020**, *14*, 1–8, doi:10.3389/fnhum.2020.00191.

95. Videnovic, A.; Metman, L.V. Deep Brain Stimulation for Parkinson's Disease: Prevalence of Adverse Events and Need for Standardized Reporting. *Movement Disorders* **2008**, *23*, doi:10.1002/mds.21753.

96. Bronstein, J.M.; Tagliati, M.; Alterman, R.L.; Lozano, A.M.; Volkmann, J.; Stefani, A.; Horak, F.B.; Okun, M.S.; Foote, K.D.; Krack, P.; et al. Deep Brain Stimulation for Parkinson Disease an Expert Consensus and Review of Key Issues. *Arch Neurol* 2011, *68*.

97. Iacopino, D.G.; Gagliardo, C.; Giugno, A.; Giammalva, G.R.; Napoli, A.; Maugeri, R.; Graziano, F.; Valentino, F.; Cosentino, G.; D'Amelio, M.; et al. Preliminary Experience with a Transcranial Magnetic Resonance–Guided Focused Ultrasound Surgery System Integrated with a 1.5-T MRI Unit in a Series of Patients with Essential Tremor and Parkinson's Disease. *Neurosurg Focus* **2018**, *44*, E7, doi:10.3171/2017.11.FOCUS17614.

98. Gerbasi, M.E.; Nambiar, S.; Reed, S.; Hennegan, K.; Hadker, N.; Eldar-Lissai, A.; Cosentino, S. Essential Tremor Patients Experience Significant Burden beyond Tremor: A Systematic Literature Review. *Front Neurol* 2022, *13*.

99. Louis, E.D.; Machado, D.G. Tremor-Related Quality of Life: A Comparison of Essential Tremor vs.Parkinson's Disease Patients. *Parkinsonism Relat Disord* **2015**, *21*, doi:10.1016/j.parkreldis.2015.04.019.

100. Heusinkveld, L.E.; Hacker, M.L.; Turchan, M.; Davis, T.L.; Charles, D. Impact of Tremor on Patients with Early Stage Parkinson's Disease. *Front Neurol* 2018, *9*.

101. Appleman, E.R.; Stavitsky, K.; Cronin-Golomb, A. Relation of Subjective Quality of Life to Motor Symptom Profile in Parkinson's Disease. *Parkinsons Dis* 2011.

102. Hariz, G.M.; Limousin, P.; Hamberg, K. "dBS Means Everything - For Some Time". Patients' Perspectives on Daily Life with Deep Brain Stimulation for Parkinson's Disease. *J Parkinsons Dis* **2016**, *6*, doi:10.3233/JPD-160799.

103. Giammalva, G.R.; Gagliardo, C.; Marrone, S.; Paolini, F.; Gerardi, R.M.; Umana, G.E.; Yağmurlu, K.; Chaurasia, B.; Scalia, G.; Midiri, F.; et al. Focused Ultrasound in Neuroscience. State of the Art and Future Perspectives. *Brain Sci* **2021**, *11*, doi:10.3390/brainsci11010084.

104. Elias, W.J.; Huss, D.; Voss, T.; Loomba, J.; Khaled, M.; Zadicario, E.; Frysinger, R.C.; Sperling, S.A.; Wylie, S.; Monteith, S.J.; et al. A Pilot Study of Focused Ultrasound Thalamotomy for Essential Tremor. *New England Journal of Medicine* **2013**, *369*, 640–648, doi:10.1056/NEJMoa1300962.

105. Napoli, A.; Anzidei, M.; Ciolina, F.; Marotta, E.; Cavallo Marincola, B.; Brachetti, G.; Di Mare, L.; Cartocci, G.; Boni, F.; Noce, V.; et al. MR-Guided High-Intensity Focused Ultrasound: Current Status of an Emerging Technology. *Cardiovasc Intervent Radiol* 2013, *36*, 1190–1203.

106. Jolesz, F.A.; McDannold, N.J. Magnetic Resonance-Guided Focused Ultrasound. A New Technology for Clinical Neurosciences. *Neurol Clin* 2014, *32*, 253–269.

107. Bauer, R.; Martin, E.; Haegele-Link, S.; Kaegi, G.; von Specht, M.; Werner, B. Noninvasive Functional Neurosurgery Using Transcranial MR Imaging-Guided Focused Ultrasound. *Parkinsonism Relat Disord* **2014**, *20*, doi:10.1016/S1353-8020(13)70046-4.

108. Schlesinger, D.; Benedict, S.; Diederich, C.; Gedroyc, W.; Klibanov, A.; Larner, J. MR-Guided Focused Ultrasound Surgery, Present and Future. *Med Phys* **2013**, *40*, 80901, doi:10.1118/1.4811136.

109. Kumar, R.; Lozano, A.M.; Sime, E.; Lang, A.E. Long-Term Follow-up of Thalamic Deep Brain Stimulation for Essential and Parkinsonian Tremor. *Neurology* **2003**, *61*, 1601–1604, doi:10.1212/01.WNL.0000096012.07360.1C.

110. Schuurman, P.R.; Bosch, D.A.; Bossuyt, P.M.M.; Bonsel, G.J.; van Someren, E.J.W.; de Bie, R.M.A.; Merkus, M.P.; Speelman, J.D. A Comparison of Continuous Thalamic Stimulation and Thalamotomy for Suppression of Severe Tremor. *New England Journal of Medicine* **2000**, *342*, 461–468, doi:10.1056/NEJM200002173420703.

111. Fishman, P.S. Thalamotomy for Essential Tremor: FDA Approval Brings Brain Treatment with FUS to the Clinic. *J Ther Ultrasound* 2017, *5*.

112. Elias, W.J.; Lipsman, N.; Ondo, W.G.; Ghanouni, P.; Kim, Y.G.; Lee, W.; Schwartz, M.; Hynynen, K.; Lozano, A.M.; Shah, B.B.; et al. A Randomized Trial of Focused Ultrasound Thalamotomy for Essential Tremor. *New England Journal of Medicine* **2016**, *375*, 730–739, doi:10.1056/NEJMoa1600159.

113. Bond, A.E.; Shah, B.B.; Huss, D.S.; Dallapiazza, R.F.; Warren, A.; Harrison, M.B.; Sperling, S.A.; Wang, X.Q.; Gwinn, R.; Witt, J.; et al. Safety and Efficacy of Focused Ultrasound Thalamotomy for Patients with Medication-Refractory, Tremor-Dominant Parkinson Disease a Randomized Clinical Trial. *JAMA Neurol* **2017**, doi:10.1001/jamaneurol.2017.3098.

114. Lipsman, N.; Schwartz, M.L.; Huang, Y.; Lee, L.; Sankar, T.; Chapman, M.; Hynynen, K.; Lozano, A.M. MR-Guided Focused Ultrasound Thalamotomy for Essential Tremor: A Proof-of-Concept Study. *Lancet Neurol* **2013**, *12*, 462–468, doi:10.1016/S1474-4422(13)70048-6.

115. Tamburin, S.; Paio, F.; Bovi, T.; Bulgarelli, G.; Longhi, M.; Foroni, R.; Mantovani, E.; Polloniato, P.M.; Tagliamonte, M.; Zivelonghi, E.; et al. Magnetic Resonance-Guided Focused Ultrasound Unilateral for Medically Refractory Essential Tremor: 3-Year-up Data. *Front. Neurol.* **2024**, *15*, 1360035.

116. Levi, V.; Eleopra, R.; Franzini, A.; Romito, L. Is Deep Brain Stimulation Still an Option for Tremor Recurrence after Focused Ultrasound Thalamotomy? A Case Report. *Journal of Clinical Neuroscience* **2019**, *68*, 344–346, doi:10.1016/j.jocn.2019.07.035.

117. Tommasino, E.; Bruno, F.; Catalucci, A.; Varrassi, M.; Sucapane, P.; Cerone, D.; Pistoia, F.; Di Cesare, E.; Barile, A.; Ricci, A.; et al. Prognostic Value of Brain Tissues' Volumes in Patients with Essential Tremor Treated with MRgFUS Thalamotomy. *Journal of Clinical Neuroscience* **2021**, *92*, doi:10.1016/j.jocn.2021.07.051.

118. Shiramba, A.; Lane, S.; Ray, N.; Gilbertson, T.; Srinivasaiah, R.; Panicker, J.; Radon, M.; Osman-Farah, J.; Macerollo, A. Efficacy and Safety of Magnetic Resonance-Guided Focused Thalamotomy in Essential Tremor: A Systematic review and Metanalysis. *Mov. Disord.* **2025**, *40*, 1020–1033.

119. Braccia, A.; Golfrè Andreasi, N.; Ghielmetti, F.; Aquino, D.; Savoldi, A.P.; Cilia, R.; Telese, R.; Colucci, F.; Gaudiano, G.; Romito, L.M.; et al. Magnetic Resonance-Guided Focused Ultrasound Thalamotomy in a prospective Cohort of 52 Patients with Parkinson's Disease: A Critical Role of Age and Lesion Volume for Predicting Relapse. *Mov. Disord.* **2025**, *40*, 478–489.

120. Bruno, F.; Badini, P.; Innocenzi Antonio and Saporito, G.; Catalucci, A.; Sucapane, P.; Barile, A.; Cesare, E. Di; Marini, C.; Pistoia, F.; Splendiani, A. Early Re-Emerging Tremor after MRgFUS Thalamotomy: Case-Control Analysis of Procedural and Imaging Features. *Front. Neurol.* **2024**, *15*, 1356613.

121. Onder, H. Recurrence of Parkinson's Disease Tremor after Focused Thalamotomy? *Mov. Disord.* **2024**, *39*, 758–759.

122. Hino, S.; Maki, F.; Yamaguchi, T.; Kaburagi, M.; Nakano, M.; Iwamuro, H.; Takasaki, M.; Iijima, K.; Kanouchi, M.; Sasanuma, J.; et al. Effectiveness and Safety of MR-Guided Focused Ultrasound Thalamotomy in Patients with Essential Tremor and Low Skull Density Ratio: A Study of 101 Cases. *J Neurosurg* **2024**, *141*, doi:10.3171/2023.11.JNS231799.

123. Hashida, M.; Maesawa, S.; Kato, S.; Nakatsubo, D.; Tsugawa, T.; Torii, J.; Tanei, T.; Ishizaki, T.; Mutoh, M.; Ito, Y.; et al. Outcomes and Prognostic Factors of Magnetic Resonance-Guided Focused Ultrasound Thalamotomy for Essential Tremor at 2-Year Follow-Up. *Neurol Med Chir (Tokyo)* **2024**, *64*, doi:10.2176/jns-nmc.2023-0202.

124. Kapadia, A.N.; Elias, G.J.B.; Boutet, A.; Germann, J.; Pancholi, A.; Chu, P.; Zhong, J.; Fasano, A.; Munhoz, R.; Chow, C.; et al. Multimodal MRI for MRgFUS in Essential Tremor: Post-Treatment Radiological Markers of Clinical Outcome. *J Neurol Neurosurg Psychiatry* **2020**, *91*, 921–927, doi:10.1136/jnnp-2020-322745.

125. Jameel, A.; Gedroyc, W.; Nandi, D.; Jones, B.; Kirmi, O.; Molloy, S.; Tai, Y.; Charlesworth, G.; Bain, P. Double Lesion MRgFUS Treatment of Essential Tremor Targeting the Thalamus and Posterior Sub-Thalamic Area: Preliminary Study with Two Year Follow-Up. *Br J Neurosurg* **2022**, *36*, doi:10.1080/02688697.2021.1958150.

126. Bruno, F.; Catalucci, A.; Varrassi, M.; Arrigoni, F.; Sucapane, P.; Cerone, D.; Pistoia, F.; Torlone, S.; Tommasino, E.; De Santis, L.; et al. Comparative Evaluation of Tractography-Based Direct Targeting and Atlas-Based Indirect Targeting of the Ventral Intermediate (Vim) Nucleus in MRgFUS Thalamotomy. *Sci Rep* **2021**, *11*, doi:10.1038/s41598-021-93058-2.

127. Bruno, F.; Tommasino, E.; Pertici, L.; Pagliei, V.; Gagliardi, A.; Catalucci, A.; Arrigoni, F.; Palumbo, P.; Sucapane, P.; Pistoia, F.; et al. MRgFUS Thalamotomy for the Treatment of Tremor: Evaluation of Learning Curve and Operator's Experience Impact on the Procedural and Clinical Outcome. *Acta Neurochir (Wien)* **2023**, *165*, doi:10.1007/s00701-023-05510-z.

128. Zur, G.; Lesman-Segev, O.H.; Schlesinger, I.; Goldsher, D.; Sinai, A.; Zaaroor, M.; Assaf, Y.; Eran, A.; Kahn, I. Tremor Relief and Structural Integrity after MRI-Guided Focused US Thalamotomy in Tremor Disorders. *Radiology* **2020**, *294*, doi:10.1148/radiol.2019191624.

129. Hasegawa, T.; Yoshida, S.; Sugeno, N.; Kobayashi, J.; Aoki, M. DnaJ/Hsp40 Family and Parkinson's Disease. *Front Neurosci* 2018, *11*.

130. Zhang, K.; Pan, H.; Zhao, Y.; Wang, Y.; Zeng, Q.; Zhou, X.; He, R.; Zhou, X.; Xiang, Y.; Zhou, Z.; et al. Genetic Analysis of HSP40/DNAJ Family Genes in Parkinson's Disease: A Large Case-Control Study. *Mol Neurobiol* **2022**, *59*, doi:10.1007/s12035-022-02920-5.

131. Witt, S.N. Molecular Chaperones, α-Synuclein, and Neurodegeneration. *Mol Neurobiol* 2013, *47*, 552–560.

132. Irwin, R.; Faust, O.; Petrovic, I.; Wolf, S.G.; Hofmann, H.; Rosenzweig, R. Hsp40s Play Complementary Roles in the Prevention of Tau Amyloid Formation. *Elife* **2021**, *10*, doi:10.7554/ELIFE.69601.

133. Lackie, R.E.; Maciejewski, A.; Ostapchenko, V.G.; Marques-Lopes, J.; Choy, W.Y.; Duennwald, M.L.; Prado, V.F.; Prado, M.A.M. The Hsp70/Hsp90 Chaperone Machinery in Neurodegenerative Diseases. *Front Neurosci* 2017, *11*.

134. Bohush, A.; Bieganowski, P.; Filipek, A. Hsp90 and Its Co-Chaperones in Neurodegenerative Diseases. *Int J Mol Sci* 2019, *20*.

135. Rane, A.; Rajagopalan, S.; Ahuja, M.; Thomas, B.; Chinta, S.J.; Andersen, J.K. Hsp90 Co-Chaperone P23 Contributes to Dopaminergic Mitochondrial Stress via Stabilization of PHD2: Implications for Parkinson's Disease. *Neurotoxicology* **2018**, *65*, doi:10.1016/j.neuro.2018.02.012.

136. Feng, M.J.; Zhang, L.; Liu, Z.; Zhou, P.; Lu, X. The Expression and Release of Hsp60 in 6-OHDA Induced in Vivo and in Vitro Models of Parkinson's Disease. *Neurochem Res* **2013**, *38*, doi:10.1007/s11064-013-1127-8.

137. Vicente Miranda, H.; Chegão, A.; Oliveira, M.S.; Fernandes Gomes, B.; Enguita, F.J.; Outeiro, T.F. Hsp27 Reduces Glycation-Induced Toxicity and Aggregation of Alpha-Synuclein. *FASEB Journal* **2020**, *34*, 6718–6728, doi:10.1096/fj.201902936R.

138. Gorman, A.M.; Szegezdi, E.; Quigney, D.J.; Samali, A. Hsp27 Inhibits 6-Hydroxydopamine-Induced Cytochrome c Release and Apoptosis in PC12 Cells. *Biochem Biophys Res Commun* **2005**, *327*, 801–810, doi:10.1016/j.bbrc.2004.12.066.

139. Navarro-Zaragoza, J.; Cuenca-Bermejo, L.; Almela, P.; Laorden, M.-L.; Herrero, M.-T. Could Small Heat Shock Protein HSP27 Be a First-Line Target for Preventing Protein Aggregation in Parkinson's Disease? **2021**, doi:10.3390/ijms.

140. Asthana, A.; Bollapalli, M.; Tangirala, R.; Bakthisaran, R.; Mohan Rao, C. Hsp27 Suppresses the Cu2+-Induced Amyloidogenicity, Redox Activity, and Cytotoxicity of α-Synuclein by Metal Ion Stripping. *Free Radic Biol Med* **2014**, *72*, 176–190, doi:10.1016/j.freeradbiomed.2014.04.012.

141. Lan, Y.L.; Zhou, J.J.; Liu, J.; Huo, X.K.; Wang, Y.L.; Liang, J.H.; Zhao, J.C.; Sun, C.P.; Yu, Z.L.; Fang, L.L.; et al. Uncaria Rhynchophylla Ameliorates Parkinson's Disease by Inhibiting HSP90 Expression: Insights from Quantitative Proteomics. *Cellular Physiology and Biochemistry* **2018**, *47*, doi:10.1159/000490837.

142. Inda, C.; Bolaender, A.; Wang, T.; Gandu, S.R.; Iii, J.K. *Stressing Out Hsp90 in Neurotoxic Proteinopathies*;

143. Waza, M.; Adachi, H.; Katsuno, M.; Minamiyama, M.; Tanaka, F.; Doyu, M.; Sobue, G. Modulation of Hsp90 Function in Neurodegenerative Disorders: A Molecular-Targeted Therapy against Disease-Causing Protein. *J Mol Med* 2006, *84*, 635–646.

144. Bohush, A.; Niewiadomska, G.; Weis, S.; Filipek, A. HSP90 and Its Novel Co-Chaperones, SGT1 and CHP-1, in Brain of Patients with Parkinson's Disease and Dementia with Lewy Bodies. *J Parkinsons Dis* **2019**, *9*, 97–107, doi:10.3233/JPD-181443.

145. Mansour, H.M.; Mohamed, A.F.; Khattab, M.M.; El-Khatib, A.S. Heat Shock Protein 90 in Parkinson's Disease: Profile of a Serial Killer. *Neuroscience* 2024, *537*, 32–46.

146. He, Y.; Wang, Z. The Roles of HSP40/DNAJ Protein Family in Neurodegenerative Diseases. *Zhejiang Da Xue Xue Bao Yi Xue Ban* 2022, *51*.

147. Rajput, A.; Ross, J.P.; Bernales, C.Q.; Rayaprolu, S.; Soto-Ortolaza, A.I.; Ross, O.A.; Van Gerpen, J.; Uitti, R.J.; Wszolek, Z.K.; Rajput, A.H.; et al. VPS35 and DNAJC13 Disease-Causing Variants in Essential Tremor. *European Journal of Human Genetics* **2015**, *23*, 887–888, doi:10.1038/ejhg.2014.164.

148. Tabassum, M.; Suman, A. Al; Suero Molina, E.; Pan, E.; Di Ieva, A.; Liu, S. Radiomics and Machine Learning in Brain Tumors and Their Habitat: A Systematic Review. *Cancers (Basel)* 2023, *15*.

149. Wisnu Wardhana, D.P.; Maliawan, S.; Mahadewa, T.G.B.; Rosyidi, R.M.; Wiranata, S. Radiomic Features as Artificial Intelligence Prognostic Models in glioblastoma: A Systematic Review and Meta-Analysis. *Diagnostics (Basel)* **2024**, *14*.

150. Nowakowski, A.; Lahijanian, Z.; Panet-Raymond, V.; Siegel, P.M.; Petrecca, K.; Maleki, F.; Dankner, M. Radiomics as an Emerging Tool in the Management of Brain Metastases. *Neurooncol Adv* 2022, *4*.

151. Tavanaei, R.; Akhlaghpasand, M.; Alikhani, A.; Hajikarimloo, B.; Ansari, A.; Yong, R.L.; Margetis, K. Performance of Radiomics-Based Machine Learning and Deep-Based Methods in the Prediction of Tumor Grade in meningioma: A Systematic Review and Meta-Analysis. *Neurosurg. Rev.* **2025**, *48*, 78.

152. Liu, J.; Shan, Y.; Gao, G. The Application Value of CT Radiomics Features in Predicting Pressure Amplitude Correlation Index in Patients with Severe Traumatic Brain Injury. *Front Neurol* **2022**, *13*, doi:10.3389/FNEUR.2022.905655.

153. Badjatia, N.; Podell, J.; Felix, R.B.; Chen, L.K.; Dalton, K.; Wang, T.I.; Yang, S.; Hu, P. Machine Learning Approaches to Prognostication in Traumatic Brain. *Curr. Neurol. Neurosci. Rep.* **2025**, *25*, 19.

154. Shi, D.; Zhang, H.; Wang, G.; Wang, S.; Yao, X.; Li, Y.; Guo, Q.; Zheng, S.; Ren, K. Machine Learning for Detecting Parkinson's Disease by Resting-State Functional Magnetic Resonance Imaging: A Multicenter Radiomics Analysis. *Front Aging Neurosci* **2022**, *14*, doi:10.3389/fnagi.2022.806828.

155. Wu, Y.; Cheng, Y.; Xiao, Y.; Shang, H.; Ou, R. The Role of Machine Learning in Cognitive Impairment in Parkinson: Systematic Review and Meta-Analysis. *J. Med. Internet Res.* **2025**, *27*, e59649.

156. Liu, Y.; Xiao, B.; Zhang, C.; Li, J.; Lai, Y.; Shi, F.; Shen, D.; Wang, L.; Sun, B.; Li, Y.; et al. Predicting Motor Outcome of Subthalamic Nucleus Deep Brain Stimulation for Parkinson's Disease Using Quantitative Susceptibility Mapping and Radiomics: A Pilot Study. *Front Neurosci* **2021**, *15*, doi:10.3389/fnins.2021.731109.

157. Zhang, D.; Xiong, Y.; Lu, H.; Duan Caohui and Huang, J.; Li, Y.; Bian, X.; Zhang, D.; Zhou, J.; Pan, L.; Lou, X. Predicting Tremor Improvement after MRgFUS Thalamotomy in essential Tremor from Preoperative Spontaneous Brain Activity: A Learning Approach. *Sci. Bull. (Beijing)* **2024**, *69*, 3098–3105.

158. Navarro-zaragoza, J.; Cuenca-bermejo, L.; Almela, P.; Laorden, M.L.; Herrero, M.T. Could Small Heat Shock Protein Hsp27 Be a First-line Target for Preventing Protein Aggregation in Parkinson's Disease? *Int J Mol Sci* 2021, *22*.

159. Ebrahimi-Fakhari, D.; Wahlster, L.; McLean, P.J. Molecular Chaperones in Parkinson's Disease - Present and Future. *J Parkinsons Dis* 2011, *1*.

160. Seasons, G.M.; Pellow, C.; Kuipers, H.F.; Pike, G.B. Ultrasound and Neuroinflammation: Immune Modulation via the Heat Response. *Theranostics* **2024**, *14*, 3150–3177.

161. Haider, T.; Simader, E.; Glück, O.; Ankersmit, H.J.; Heinz, T.; Hajdu, S.; Negrin, L.L. Systemic Release of Heat-Shock Protein 27 and 70 Following Severe Trauma. *Sci Rep* **2019**, *9*, doi:10.1038/s41598-019-46034-w.

162. Erekat, N.; Al-Khatib, A.; Al-Jarrah, M. Heat Shock Protein 90 Is a Potential Therapeutic Target for Ameliorating Skeletal Muscle Abnormalities in Parkinson's Disease. *Neural Regen Res* **2014**, *9*, doi:10.4103/1673-5374.130105.

163. Svirsky, S.E.; Li, Y.; Henchir, J.; Rodina, A.; Carlson, S.W.; Chiosis, G.; Dixon, C.E. Experimental Traumatic Brain Injury Increases Epichaperome Formation. *Neurobiol Dis* **2023**, *188*, doi:10.1016/j.nbd.2023.106331.

164. Luo, W.; Sun, W.; Taldone, T.; Rodina, A.; Chiosis, G. Heat Shock Protein 90 in Neurodegenerative Diseases. *Mol Neurodegener* 2010, *5*.

165. Kishinevsky, S.; Wang, T.; Rodina, A.; Chung, S.Y.; Xu, C.; Philip, J.; Taldone, T.; Joshi, S.; Alpaugh, M.L.; Bolaender, A.; et al. HSP90-Incorporating Chaperome Networks as Biosensor for Disease-Related Pathways in Patient-Specific Midbrain Dopamine Neurons. *Nat Commun* **2018**, *9*, doi:10.1038/s41467-018-06486-6.

166. Joshi, N.; Raveendran, A.; Nagotu, S. Chaperones and Proteostasis: Role in Parkinson's Disease. *Diseases* 2020, *8*.

167. Foster, J.A.; Brown, I.R. Differential Induction of Heat Shock MRNA in Oligodendrocytes, Microglia, and Astrocytes Following Hyperthermia. *Molecular Brain Research* **1997**, *45*, doi:10.1016/S0169-328X(96)00138-6.

168. Chaudhury, S.; Keegan, B.M.; Blagg, B.S.J. The Role and Therapeutic Potential of Hsp90, Hsp70, and Smaller Heat Shock Proteins in Peripheral and Central Neuropathies. *Med Res Rev* 2021, *41*.

169. Wang, B.; Liu, Y.; Huang, L.; Chen, J.; Li, J.J.; Wang, R.; Kim, E.; Chen, Y.; Justicia, C.; Sakata, K.; et al. A CNS-Permeable Hsp90 Inhibitor Rescues Synaptic Dysfunction and Memory Loss in APP-Overexpressing Alzheimer's Mouse Model via an HSF1-Mediated Mechanism. *Mol Psychiatry* **2017**, *22*, doi:10.1038/mp.2016.104.

170. Gerges, N.Z.; Tran, I.C.; Backos, D.S.; Harrell, J.M.; Chinkers, M.; Pratt, W.B.; Esteban, J.A. Independent Functions of Hsp90 in Neurotransmitter Release and in the Continuous Synaptic Cycling of AMPA Receptors. *Journal of Neuroscience* **2004**, *24*, doi:10.1523/JNEUROSCI.0594-04.2004.

171. Taha, B.; Boley, D.; Sun, J.; Chen, C. Potential and Limitations of Radiomics in Neuro-Oncology. *Journal of Clinical Neuroscience* 2021, *90*.

172. Gerardi, R.M.; Cannella, R.; Bonosi, L.; Vernuccio, F.; Ferini, G.; Viola, A.; Zagardo, V.; Buscemi, F.; Costanzo, R.; Porzio, M.; et al. Forecasting Molecular Features in IDH-Wildtype Gliomas: The State of the Art of Radiomics Applied to Neurosurgery. *Cancers (Basel)* 2023, *15*.

173. Taha, B.; Boley, D.; Sun, J.; Chen, C.C. State of Radiomics in Glioblastoma. *Neurosurgery* 2021, *89*.

174. Li, G.; Li, L.; Li, Y.; Qian, Z.; Wu, F.; He, Y.; Jiang, H.; Li, R.; Wang, D.; Zhai, Y.; et al. An MRI Radiomics Approach to Predict Survival and Tumour-Infiltrating Macrophages in Gliomas. *Brain* **2022**, *145*, doi:10.1093/brain/awab340.

175. Zheng, R. zhe; Zhao, Z. jie; Yang, X. tao; Jiang, S. wei; Li, Y. de; Li, W. jie; Li, X. hui; Zhou, Y.; Gao, C. jin; Ma, Y. bin; et al. Initial CT-Based Radiomics Nomogram for Predicting in-Hospital Mortality in Patients with Traumatic Brain Injury: A Multicenter Development and Validation Study. *Neurological Sciences* **2022**, *43*, doi:10.1007/s10072-022-05954-8.

176. Luo, X.; Lin, D.; Xia, S.; Wang, D.; Weng, X.; Huang, W.; Ye, H. Machine Learning Classification of Mild Traumatic Brain Injury Using Whole-Brain Functional Activity: A Radiomics Analysis. *Dis Markers* **2021**, *2021*, doi:10.1155/2021/3015238.

177. Shih, Y.J.; Liu, Y.L.; Chen, J.H.; Ho, C.H.; Yang, C.C.; Chen, T.Y.; Wu, T.C.; Ko, C.C.; Zhou, J.T.; Zhang, Y.; et al. Prediction of Intraparenchymal Hemorrhage Progression and Neurologic Outcome in Traumatic Brain Injury Patients Using Radiomics Score and Clinical Parameters. *Diagnostics (Basel)* **2022**, *12*, doi:10.3390/DIAGNOSTICS12071677.

8 Supplementary materials

Supplement 1

		HSP90_T0	HSP90_T1	HSP90_T2	HSP40_T0	HSP40_T1	HSP40_T2	dHSP90_T1_T0	dHSP90_T2_T0	dHSP90_T2_T1	dHSP40_T1_T0	dHSP40_T2_T0	dHSP40_T2_T1
HSP90_T0	**Spearman's rho**	—											
	p-value	—											
HSP90_T1	**Spearman's rho**	**0.538***	—										
	p-value	**0.050**	—										
HSP90_T2	**Spearman's rho**	**0.793****	**0.640***	—									
	p-value	**0.001**	**0.016**	—									
HSP40_T0	**Spearman's rho**	-0.310	-0.002	-0.455	—								
	p-value	0.281	1.000	0.104	—								
HSP40_T1	**Spearman's rho**	-0.126	0.093	-0.341	**0.742****	—							
	p-value	0.683	0.765	0.255	**0.005**	—							
HSP40_T2	**Spearman's rho**	-0.112	-0.086	-0.279	**0.802*****	**0.714****	—						
	p-value	0.704	0.773	0.333	**<.001**	**0.008**	—						
dHSP90_T1_T0	**Spearman's rho**	**-0.692****	0.042	-0.354	0.160	-0.071	-0.130	—					
	p-value	**0.008**	0.892	0.215	0.584	0.821	0.660	—					
dHSP90_T2_T0	**Spearman's rho**	**-0.657***	-0.182	-0.169	-0.046	-0.368	-0.165	**0.820*****	—				
	p-value	**0.013**	0.532	0.563	0.880	0.217	0.573	**<.001**	—				
dHSP90_T2_T1	**Spearman's rho**	0.064	-0.187	0.345	-0.464	-0.341	-0.182	-0.152	0.213	—			
	p-value	0.832	0.522	0.227	0.097	0.255	0.532	0.605	0.464	—			
dHSP40_T1_T0	**Spearman's rho**	0.126	0.198	0.038	-0.269	0.407	-0.176	-0.104	-0.335	0.016	—		
	p-value	0.683	0.517	0.906	0.373	0.170	0.566	0.737	0.263	0.964	—		
dHSP40_T2_T0	**Spearman's rho**	0.349	0.077	0.209	0.051	0.357	**0.596***	-0.371	-0.301	0.156	0.264	—	
	p-value	0.221	0.797	0.473	0.868	0.232	**0.028**	0.192	0.295	0.594	0.383	—	
dHSP40_T2_T1	**Spearman's rho**	0.126	-0.203	0.060	0.126	-0.264	0.385	-0.132	0.143	0.060	**-0.725****	0.368	—
	p-value	0.683	0.505	0.849	0.683	0.383	0.196	0.669	0.643	0.849	**0.007**	0.217	—

Note. * p < .05, ** p < .01, *** p < .001

Supplement 1 *Correlation matrix between HSPs expression and HSPs variation (ΔHSP) in the whole population of ET and PD patients*

Supplement 2

		HSP90_T0	HSP90_T1	HSP90_T2	HSP40_T0	HSP40_T1	HSP40_T2	dHSP90_T1_T0	dHSP90_T2_T0	dHSP90_T2_T1	dHSP40_T1_T0	dHSP40_T2_T0	dHSP40_T2_T1	dHand_T1_T0	dHand_T2_T0	dHand_T2_T1	dCRST_T1_T0	dCRST_T2_T0	dCRST_T2_T1
HSP90_T0	**Spearman's rho**	—																	
	p-value	—																	
HSP90_T1	**Spearman's rho**	0.571	—																
	p-value	0.200	—																
HSP90_T2	**Spearman's rho**	0.750	0.429	—															
	p-value	0.066	0.354	—															
HSP40_T0	**Spearman's rho**	**-0.786***	-0.321	**-0.786***	—														
	p-value	**0.048**	0.498	**0.048**	—														
HSP40_T1	**Spearman's rho**	**-0.786***	-0.107	-0.679	0.571	—													
	p-value	**0.048**	0.840	0.110	0.200	—													
HSP40_T2	**Spearman's rho**	**-0.821***	-0.393	-0.607	0.750	**0.786***	—												
	p-value	**0.034**	0.396	0.167	0.066	**0.048**	—												
dHSP90_T1_T0	**Spearman's rho**	-0.393	0.357	-0.286	0.393	0.429	0.143	—											
	p-value	0.396	0.444	0.556	0.396	0.354	0.783	—											
dHSP90_T2_T0	**Spearman's rho**	-0.571	-0.179	-0.036	0.429	0.321	0.571	0.500	—										
	p-value	0.200	0.713	0.963	0.354	0.498	0.200	0.267	—										
dHSP90_T2_T1	**Spearman's rho**	0.214	-0.500	0.250	-0.321	-0.429	0.000	-0.679	0.036	—									
	p-value	0.662	0.267	0.595	0.498	0.354	1.000	0.110	0.963	—									
dHSP40_T1_T0	**Spearman's rho**	0.321	0.429	0.357	-0.679	0.179	-0.286	-0.071	-0.357	-0.179	—								
	p-value	0.498	0.354	0.444	0.110	0.713	0.556	0.906	0.444	0.713	—								
dHSP40_T2_T0	**Spearman's rho**	0.143	0.000	0.321	-0.464	0.143	0.214	-0.393	0.107	0.571	0.536	—							
	p-value	0.783	1.000	0.498	0.302	0.783	0.662	0.396	0.840	0.200	0.236	—							
dHSP40_T2_T1	**Spearman's rho**	0.036	-0.286	0.107	0.107	-0.179	0.393	-0.464	0.321	**0.786***	-0.429	0.500	—						
	p-value	0.963	0.556	0.840	0.840	0.713	0.396	0.302	0.498	**0.048**	0.354	0.267	—						

Supplement 2

		HSP90_T0	HSP90_T1	HSP90_T2	HSP40_T0	HSP40_T1	HSP40_T2	dHSP90_T1_T0	dHSP90_T2_T0	dHSP90_T2_T1	dHSP40_T1_T0	dHSP40_T2_T0	dHSP40_T2_T1	dHand_T1_T0	dHand_T2_T0	dHand_T2_T1	dCRST_T1_T0	dCRST_T2_T0	dCRST_T2_T1
dHand_T1_T0	**Spearman's rho**	-0.109	-0.218	-0.509	0.582	-0.109	0.073	-0.145	-0.346	-0.164	-0.673	-0.709	0.018	—					
	p-value	0.816	0.638	0.243	0.170	0.816	0.877	0.756	0.448	0.726	0.098	0.074	0.969	—					
dHand_T2_T0	**Spearman's rho**	0.234	0.559	-0.180	0.252	0.144	0.180	0.018	-0.252	-0.198	-0.072	0.018	0.252	0.376	—				
	p-value	0.613	0.192	0.699	0.585	0.758	0.699	0.969	0.585	0.670	0.878	0.969	0.585	0.406	—				
dHand_T2_T1	**Spearman's rho**	0.703	**0.955*** **	0.432	-0.414	-0.252	-0.487	0.234	-0.288	-0.288	0.378	0.072	-0.144	-0.183	0.609	—			
	p-value	0.078	**<.001**	0.333	0.355	0.585	0.268	0.613	0.531	0.531	0.403	0.878	0.758	0.694	0.147	—			
dCRST_T1_T0	**Spearman's rho**	0.071	-0.286	-0.357	0.036	-0.214	-0.107	-0.071	-0.179	0.500	-0.357	0.000	0.321	0.236	0.108	-0.018	—		
	p-value	0.906	0.556	0.444	0.963	0.662	0.840	0.906	0.713	0.267	0.444	1.000	0.498	0.610	0.818	0.969	—		
dCRST_T2_T0	**Spearman's rho**	0.286	0.179	-0.321	-0.036	-0.143	-0.250	0.071	-0.429	0.143	-0.107	-0.071	0.071	0.273	0.468	0.414	**0.857***	—	
	p-value	0.556	0.713	0.498	0.963	0.783	0.595	0.906	0.354	0.783	0.840	0.906	0.906	0.554	0.289	0.355	**0.024**	—	
dCRST_T2_T1	**Spearman's rho**	0.714	**0.857***	0.500	-0.536	-0.250	-0.607	0.000	-0.571	-0.464	0.607	-0.036	-0.464	-0.109	0.396	**0.811***	-0.393	0.071	—
	p-value	0.088	**0.024**	0.267	0.236	0.595	0.167	1.000	0.200	0.302	0.167	0.963	0.302	0.816	0.379	**0.027**	0.396	0.906	—

Note. * p < .05, ** p < .01, *** p < .001

Supplement 2 *Correlation matrix between HSPs expression, HSPs variation (ΔHSP) and variation of clinical score (ΔHand, ΔCRST) in ET subgroup*

Supplement 3

		HSP90_T0	HSP90_T1	HSP90_T2	HSP40_T0	HSP40_T1	HSP40_T2	dHSP90_T1_T0	dHSP90_T2_T0	dHSP90_T2_T1	dHSP40_T1_T0	dHSP40_T2_T0	dHSP40_T2_T1	dUPDRS_T1_T0	dUPDRS_T2_T0	dUPDRS_T2_T1
HSP90_T0	**Spearman's rho**	—														
	p-value	—														
HSP90_T1	**Spearman's rho**	0.321	—													
	p-value	0.498	—													
HSP90_T2	**Spearman's rho**	0.393	**0.964****	—												
	p-value	0.396	**0.003**	—												
HSP40_T0	**Spearman's rho**	0.536	0.000	-0.143	—											
	p-value	0.236	1.000	0.783	—											
HSP40_T1	**Spearman's rho**	0.714	0.143	0.143	0.829	—										
	p-value	0.136	0.803	0.803	0.058	—										
HSP40_T2	**Spearman's rho**	0.321	0.036	-0.107	**0.893***	0.543	—									
	p-value	0.498	0.963	0.840	**0.012**	0.297	—									
dHSP90_T1_T0	**Spearman's rho**	**-0.964****	-0.143	-0.214	-0.571	-0.600	-0.357	—								
	p-value	**0.003**	0.783	0.662	0.200	0.242	0.444	—								
dHSP90_T2_T0	**Spearman's rho**	**-0.929****	-0.107	-0.143	-0.679	-0.600	-0.429	**0.964****	—							
	p-value	**0.007**	0.840	0.783	0.110	0.242	0.354	**0.003**	—							
dHSP90_T2_T1	**Spearman's rho**	-0.321	0.143	0.214	-0.429	-0.086	-0.179	0.500	0.536	—						
	p-value	0.498	0.783	0.662	0.354	0.919	0.713	0.267	0.236	—						
dHSP40_T1_T0	**Spearman's rho**	0.543	0.314	0.314	0.200	0.600	-0.143	-0.314	-0.314	0.314	—					
	p-value	0.297	0.564	0.564	0.714	0.242	0.803	0.564	0.564	0.564	—					
dHSP40_T2_T0	**Spearman's rho**	0.286	0.071	-0.036	**0.786***	0.314	**0.964****	-0.321	-0.393	-0.071	-0.200	—				
	p-value	0.556	0.906	0.963	**0.048**	0.564	**0.003**	0.498	0.396	0.906	0.714	—				
dHSP40_T2_T1	**Spearman's rho**	-0.371	-0.486	-0.486	0.029	-0.486	0.314	0.086	0.086	-0.429	**-0.943***	0.371	—			
	p-value	0.497	0.356	0.356	1.000	0.356	0.564	0.919	0.919	0.419	**0.017**	0.497	—			
dUPDRS_T1_T0	**Spearman's rho**	-0.607	-0.536	-0.429	-0.643	-0.771	-0.393	0.500	0.643	0.286	-0.714	-0.321	0.600	—		
	p-value	0.167	0.236	0.354	0.139	0.103	0.396	0.267	0.139	0.556	0.136	0.498	0.242	—		
dUPDRS_T2_T0	**Spearman's rho**	-0.679	0.143	0.179	-0.679	-0.657	-0.286	0.714	**0.821***	0.607	-0.543	-0.143	0.314	0.679	—	
	p-value	0.110	0.783	0.713	0.110	0.175	0.556	0.088	**0.034**	0.167	0.297	0.783	0.564	0.110	—	

Supplement 3

		HSP90_T0	HSP90_T1	HSP90_T2	HSP40_T0	HSP40_T1	HSP40_T2	dHSP90_T1_T0	dHSP90_T2_T0	dHSP90_T2_T1	dHSP40_T1_T0	dHSP40_T2_T0	dHSP40_T2_T1	dUPDRS_T1_T0	dUPDRS_T2_T0	dUPDRS_T2_T1
dUPDRS_T2_T1	**Spearman's rho**	-0.546	0.236	0.309	-0.709	-0.725	-0.327	0.600	0.727	0.636	-0.522	-0.164	0.290	0.636	**0.982*** **	—
	p-value	0.205	0.610	0.500	0.074	0.103	0.474	0.154	0.064	0.124	0.288	0.726	0.577	0.124	**<.001**	—

Note. * p < .05, ** p < .01, *** p < .001

Supplement 3 *Correlation matrix between HSPs expression, HSPs variation (ΔHSP) and variation of clinical score (ΔUPDRS) in PD subgroup*